

N71-34496

LA-4714-MS

COPY

CMB-13 Research on Carbon and Graphite

Report No. 16

Summary of Progress from November 1, 1970 to January 31, 1971

CASE FILE
COPY



los alamos
scientific laboratory
of the University of California
LOS ALAMOS, NEW MEXICO 87544

This report was prepared as an account of work sponsored by the United States Government. Neither the United States nor the United States Atomic Energy Commission, nor any of their employees, nor any of their contractors, subcontractors, or their employees, makes any warranty, express or implied, or assumes any legal liability or responsibility for the accuracy, completeness or usefulness of any information, apparatus, product or process disclosed, or represents that its use would not infringe privately owned rights.

This LA. .MS report presents the summary of progress of CMF-13 research on carbon and graphite at LASL. The four most recent Summary of Progress Reports in this series, all unclassified, are:

LA-4417-MS
LA-4480-MS

LA-4526-MS
LA-4631-MS

This report, like other special-purpose documents in the LA. .MS series, has not been reviewed or verified for accuracy in the interest of prompt distribution.



LA-4714-MS
SPECIAL DISTRIBUTION
ISSUED: July 1971

CMB-13 Research on Carbon and Graphite

Report No. 16

Summary of Progress from November 1, 1970 to January 31, 1971

by

Morton C. Smith

CMB-13 RESEARCH ON CARBON AND GRAPHITE

REPORT NO. 16: SUMMARY OF PROGRESS FROM NOVEMBER 1, 1970 TO JANUARY 31, 1971

by

Morton C. Smith

I. INTRODUCTION

This is the sixteenth in a series of progress reports devoted to carbon and graphite research in LASL Group CMB-13 (formerly "CMF-13"), and summarizes work done during the months of November and December, 1970, and January, 1971. It should be understood that in such a progress report many of the data are preliminary, incomplete, and subject to correction, and many of the opinions and conclusions are tentative and subject to change. This report is intended only to provide up-to-date background information to those who are interested in the materials and programs described in it, and should not be quoted or used as a reference publicly or in print.

Research and development on carbon and graphite were undertaken by CMB-13 primarily to increase understanding of their properties and behavior as engineering materials, to improve the raw materials and processes used in their manufacture, and to learn how to produce them with consistent, predictable, useful combinations of properties. The approach taken is microstructural, based on study and characterization of natural, commercial, and experimental carbons and graphites by such techniques as x-ray diffraction, electron and optical microscopy, and porosimetry. Physical and mechanical properties are measured as functions of formulation, treatment, and environmental variables, and correlations are sought among properties and structures. Raw materials and manufacturing techniques are investigated, improved, and varied systematically in an effort to create specific internal

structures believed to be responsible for desirable combinations of properties. Prompt feedback of information among these activities then makes possible progress in all of them toward their common goal of understanding and improving manufactured carbons and graphites.

Since its beginning, this research has been sponsored by the Division of Space Nuclear Systems of the United States Atomic Energy Commission, through the Space Nuclear Propulsion Office. More recently additional general support for it has been provided by the Office of Advanced Research and Technology of the National Aeronautics and Space Administration. Many of its facilities and services have been furnished by the Division of Military Application of AEC. The direct and indirect support and the guidance and encouragement of these agencies of the United States Government are gratefully acknowledged.

II. SANTA MARIA COKE

A. Previous Work

Investigations of Santa Maria coke and of molded and extruded graphites made from it have previously been discussed in Reports 9 through 15 in this series.

B. Grinding Behavior (R. J. Imprescia, H. D. Lewis)

Four samples of green Santa Maria coke were heat-treated at very low temperatures, ground by a standard ("S+T+I") schedule involving two stages of hammer milling and one of fluid-energy milling, and characterized, with the results shown in Table I. Lot CP-19 was simply dried at 110°C. Lots CP-20, CP-21, and CP-22 were

TABLE I
PARTICLE CHARACTERISTICS OF SANTA MARIA GRINDING PRODUCTS

	CMB-13 Lot No.							
	CP-19	CP-20	CP-21	CP-22	13-5 ^(e)	G-35 ^(f)	G-35 ^(g)	G-26
Ht. -Trt. Temp., °C	Green ^(a)	600	700	810	1500	2500	2500	2500
Helium Density, g/cm ³	1.375	1.392	1.448	1.470	2.155	2.117	2.113	2.084
Micromerograph Statistics ^(b)								
\bar{x}_3	2.869	3.551	4.175	3.915	2.704	3.190	3.072	3.317
s_{x3}^2	1.534	2.166	1.626	2.146	1.281	2.476	2.162	---
\bar{x}	0.036	0.379	0.372	0.272	0.444	-0.035	-0.037	0.218
s_x^2	0.192	0.181	0.268	0.162	0.149	0.185	0.185	0.177
\bar{d}_3 , microns	31.95	78.92	118.0	104.5	24.18	68.21	46.21	57.55
s_{d3}^2 , microns ²	899.8	9551	13,911	12,579	366.0	16,122	2344	---
\bar{d} , microns	1.20	1.66	1.76	1.49	1.735	1.10	1.09	1.41
s_d^2 , microns ²	1.07	1.63	3.20	1.36	1.508	0.641	0.640	1.05
g_d	13.9	36.6	118.6	39.4	20.8	9.69	9.28	---
S_W , cm ² /g	5547	3787	1811	2921	3681	3911	4047	3181
CV _d	0.86	0.77	1.02	0.78	0.71	0.73	0.73	0.73
BET Surface Area								
S_W , m ² /g	4.14	4.70	4.50	4.65	27.72	4.51	4.55	4.43
s_S	---	0.23	0.30	0.10	0.32	0.13	0.01	0.31
d_s (c)	1.05	0.92	0.92	0.88	0.10	0.63	0.62	0.65
Fuzziness Ratio ^(d)	7.5	12.4	24.8	15.9	75.3	11.5	11.2	13.9

(a) Coked at 450-500°C, dried at 110°C.

(b) Interval model.

(c) $d_s = 6/\rho S_W$.

(d) BET surface area divided by that calculated from Micromerograph data.

(e) Y-12 designation.

(f) As-received.

(g) Minus 50 mesh fraction.

calcined at 600, 700, and 810°C respectively. All four samples contained residual volatiles and, during vacuum, outgassing at 380°C prior to surface-area measurements, produced a dark red-orange to black deposit in the neck of the sample tube.

Particle-size data are summarized in Table I and plotted in Fig. 1. All data were corrected for the presence of material coarser than 300 μ , which is the upper limit of resolution of the Micromerograph. (However, both corrected and uncorrected data are plotted for Lot

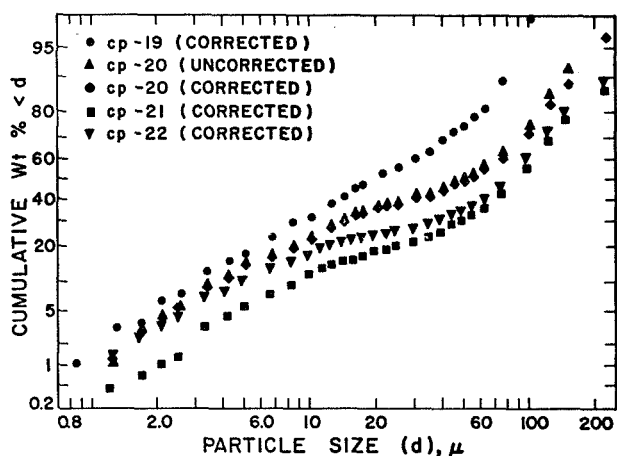


Fig. 1. Micromerograph particle-size data for Santa Maria fillers heat-treated at very low temperatures.

CP-20.) Both the sample statistics and the curves show progressive coarsening of the grinding product (reduced grindability) as a result of pre-grind heat-treatments to 600 and 700°C, and a reversal of this trend (increased grindability) from heat-treatment to 810°C. As was discussed in Report No. 15, pp 6-7, the trend of decreasing particle size with increasing calcining temperature then continues to higher temperature.

The BET surface areas, S_w , listed in Table I are more nearly alike than would be expected from the particle-size data for these four samples. However, this may result from measurement errors caused by volatile substances condensed in the neck of the sample tube. The fuzziness ratios listed are correspondingly uncertain.

A sample of purified Santa Maria coke which had been calcined at 1500°C and ground at the Union Carbide Y-12 Plant, was obtained from LASL Group CMB-6. It was identified by them as Y-12 Lot 13-5. Particle characteristics are summarized in Table I, and particle-size data are plotted in Fig. 13. This was a much finer flour than either the four grinding products described above or a flour produced here by grinding a coke calcined at 1470°C (described in Report No. 15, pp 6-7). At least in part, the latter difference undoubtedly results from a difference in the grinding procedures used.

Another lot of "Blend 1" Santa Maria graphite flour has been obtained from the Y-12 Plant and identified as

CMB-13 Lot G-35. Presumably it has been graphitized at 2500°C and is a duplicate of a previous "Blend 1" shipment identified as CMB-13 Lot G-26. The two lots are compared in Table I. Since Lot G-35 contained particles coarser than 1 mm dia it was screened through 50 mesh (300 μ) for Micromerograph analysis. Both corrected ("as-received") and uncorrected ("minus 50 mesh") data are listed. The new Lot G-35 flour is distinctly finer than the older Lot G-26 flour, as was discussed in Report No. 15 (pp 1-2) on the basis of sieve analyses. In other respects the two lots are quite similar.

C. Molded Graphites (R. J. Imprescia)

Several series of hot-molded graphites have been made from hammer-milled Santa Maria LV coke, which had been calcined by its manufacturer at about 1090°C. The variables examined were: binder type and concentration; molding pressure; and the proportion of Thermax carbon black added to the mix.

Two batches of LV coke filler were produced for these experiments by identical grinding methods, and were identified as Lots CP-17 and CP-17b. They have been compared in Report No. 14 in this series, and are nearly identical. All graphites were made by standard hot-molding ("pressure-baking") techniques, which were also described in Report No. 14.

1. Binder Type and Concentration, Molding Pressure:

The graphites of Series 65, whose properties are listed in Table II, were all made using Lot CP-17 filler. Their manufacture was described in detail in Report No. 14.

Specimens 65A-3 and 65C-2 were made using Barrett Grade 23S coal-tar pitch, whose softening point is 54°C. Since Barrett Grade 30MH pitch, whose softening point is 110°C, produced higher graphite densities, all subsequent moldings were made with the 30MH pitch. It is of interest, however, that graphites made from the 23S pitch appeared to have higher thermal expansion coefficients than did those made from 30MH pitch.

So long as an excess of binder was present in the mix, the calculated optimum binder concentration (which indicates the efficiency of filler-particle packing) and the density properties were essentially constant for a given

TABLE II
PROPERTIES OF HOT MOLDED SANTA MARIA GRAPHITES, SERIES 65

SPECIMEN NO:	65C-2	65A-3	65D-1	65D-2	65D-3	65B-1	65B-2	65B-3	65E-1b	65E-2	65E-3
Binder Conc. ^(a) , pph	20	30	20	20	20	30	30	30	40	40	40
Binder Opt., pph	19.3	18.8	19.0	31.9	38.6	18.1	22.8	24.8	19.3	22.8	26.1
Molding Pressure, psi	4000	4000	4000	1500	500	4000	1500	500	4000	1500	500
Density, g/cm ³	1.694	1.739	1.742	1.699	1.592	1.770	1.736	1.710	1.771	1.746	1.710
Tensile Str., psi											
With-grain	2038	---	3518	2651	1511	3672	3426	3220	3073	3517	2587
Compr. Str., psi											
With-grain	8927	11,430	12,015	10,267	6254	12,609	11,963	11,912	12,492	12,601	10,978
Across-grain	10,384	11,862	12,269	10,576	7188	13,347	12,653	11,865	12,938	13,163	11,752
Flexure Str., psi											
With-grain	3346	3876	4671	4393	2886	5326	5112	4929	4244	5048	5000
Across-grain	3599	4674	5171	4841	2729	5302	5322	5299	4825	5080	4814
CTE, x 10 ⁻⁶ /°C ^(b)											
With-grain	6.17	6.30	5.28	5.12	4.89	5.69	5.23	5.08	5.10	5.21	5.15
Across-grain	5.65	5.97	5.77	5.36	5.24	5.93	5.37	5.15	5.47	5.78	5.96
Resistivity, μΩ cm											
With-grain	1494	1381	1250	1285	1653	1184	1258	1274	1208	1268	1273
Across-grain	1500	1370	1263	1281	1514	1221	1277	1274	1249	1278	1307
Therm. Cond., W/cm°C											
With-grain	0.90	0.96	1.03	1.08	0.87	1.12	1.10	1.13	1.08	1.01	1.01
Across-grain	0.87	0.96	0.99	1.10	0.87	0.96	1.06	1.07	1.04	1.03	1.03
Young's Mod., 10 ⁶ psi											
With-grain	1.09	---	1.21	1.19	0.893	1.38	1.29	1.23	1.25	1.31	1.19
Across-grain	1.17	1.28	1.28	1.22	0.897	1.36	1.30	1.22	1.33	1.34	1.22
Anisotropies											
BAF ^(c)	1.017	1.016	1.022	~1.000	1.008	1.027	1.027	1.010	1.016	1.012	1.012
Compr. Str.	1.16	1.04	1.02	1.03	1.15	1.06	1.06	1.00	1.04	1.04	1.07
Flexure Str.	0.93	0.83	0.90	0.91	1.06	1.00	0.96	0.93	0.88	0.99	1.04
CTE	0.92	0.95	1.09	1.05	1.07	1.04	1.03	1.01	1.07	1.11	1.16
Resistivity	1.00	0.99	1.01	1.00	0.92	1.03	1.02	1.00	1.03	1.01	1.03
Therm. Cond.	1.03	1.00	1.04	0.98	1.00	1.17	1.04	1.06	1.04	0.98	0.98
Young's Mod.	0.93	---	0.95	0.98	1.00	1.01	0.99	1.01	0.94	0.98	0.98

(a) Specimens 65A-3 and 65C-2 were made with Barrett 23S pitch; all others with Barrett 30MH.

(b) Coefficient of Thermal Expansion, average, 25-645°C.

molding pressure, and did not vary significantly with binder concentration. For binder-deficient mixes, however, densities were lower and calculated binder optima were greater. Shrinkage of the molded specimens between the baked and the graphitized conditions was independent of the binder softening point, binder concentra-

tion, and molding pressure.

Microscopic examination of the Series 65 graphites revealed the typical Santa Maria structure, with no preferred orientation of particles or overall optical anisotropy.

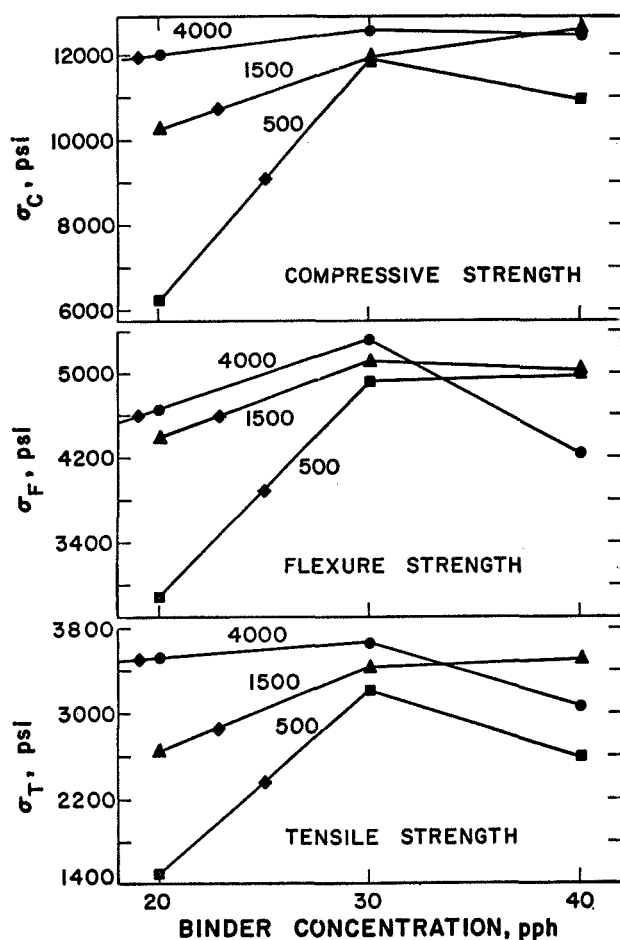


Fig. 2. With-grain properties of Series 65 graphites as functions of binder concentration for molding pressures of 500, 1500, and 4000 psi.

With-grain properties of the graphites made with 30 MH pitch are plotted in Fig. 2 and 3 as functions of binder concentration and molding pressure. The circled X's on each curve are not data points, but simply represent the binder concentration which, from mixes containing excess binder, were calculated to be optimum. Young's modulus values have not been plotted, but are listed in Table II. They ranged from about 0.9 to about 1.4×10^6 psi, and varied with binder concentration much as did the strength properties.

At a given molding pressure, variations in binder concentration had very little effect on density, so long as there was not a deficiency of binder. This was not true of the other properties investigated, which in general

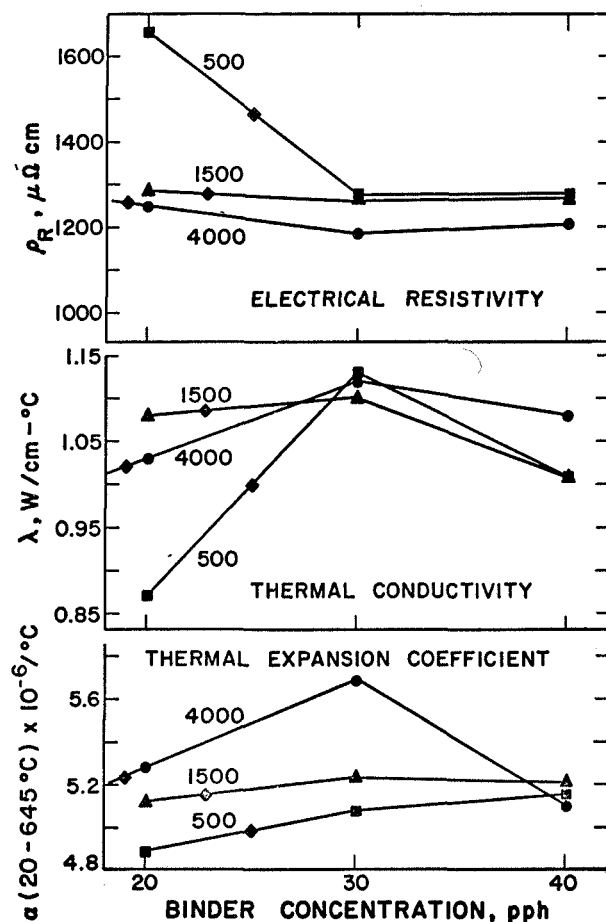


Fig. 3. With-grain properties of Series 65 graphites as functions of binder concentration for molding pressures of 500, 1500, and 4000 psi.

were quite sensitive to binder concentration--whether or not there was an excess of binder in the mix. From the curves of Fig. 2 and 3 it appears that, regardless of molding pressure, a binder concentration of about 30 pph generally represents an optimum for the enhancement of properties, and that this is considerably greater than the calculated optimum concentrations required for void filling in the packed filler. At 30 pph most of the properties curves pass through maxima or minima and, within a range of about 10%, most of the properties are essentially independent of molding pressure. The exception is thermal expansion coefficient, which increases by about 15% as molding pressure is increased from 500 to 4000 psi. At binder concentrations below 30 pph, increasing

TABLE III
EFFECT OF THERMAX ON HOT-MOLDED SANTA MARIA GRAPHITES, SERIES 71

SPECIMEN NO:	65B-1	71C-1	71A-1	71B-1
Thermax in Filler, wt. %	0	5	10	15
Density, g/cm ³	1.770	1.790	1.797	1.818
Tensile Str., psi				
With-grain	3672	3102	---	---
Compr. Str., psi				
With-grain	12,609	14,274	---	15,401
Across-grain	13,347	14,306	14,563	15,480
Flexure Str., psi				
With-grain	5326	5380	3606 ^(a)	4652
Across-grain	5302	5303	4733	4447
CTE, x 10 ⁻⁶ /°C ^(b)				
With-grain	5.69	5.94	5.76	5.82
Across-grain	5.93	6.09	6.08	5.75
Resistivity, μΩ cm				
With-grain	1184	1617	1794	1501
Across-grain	1221	1653	1839	1490
Therm. Cond., W/cm°C				
With-grain	1.12	0.87	0.80	0.73
Across-grain	0.96	0.92	0.81	0.77
Young's Mod., 10 ⁶ psi				
With-grain	1.38	1.456	1.431	1.539
Across-grain	1.37	1.425	1.444	1.550
Anisotropies				
BAF ^(c)	1.027	1.017	1.015	1.015
Compr. Str.	1.06	1.00	---	1.01
Flexure Str.	1.00	1.01	0.76	1.05
CTE	1.04	1.03	1.06	0.99
Resistivity	1.03	1.02	1.03	0.99
Therm. Cond.	1.16	0.94	0.99	0.95
Young's Mod.	1.01	1.02	0.99	0.99

(a) One test specimen only.

(b) Coefficient of Thermal Expansion, average, 25-645°C.

(c) Bacon Anisotropy Factor, σ_{oz}/σ_{ox} .

molding pressure enhances properties; at higher concentrations, there is no consistent relation between molding pressure and properties.

No gross defects were observed in these graphites. Microcracks were observed, which in some cases (graphites 65A-3 and 65B-3) nearly outlined some of the larger filler particles. In most specimens microporosity was

extensive, frequently appearing as loose aggregates of binder residue plus fines in some of the regions between large filler particles. At 30 pph of 30MH binder, properties were typical of well-mixed, good quality, Santa Maria graphites. Tensile strengths ranged up to about 3700 psi, flexure strengths to about 5000 psi, and compressive strengths to about 13,000 psi. Electrical resistivities were as low as about $1200 \mu\Omega\text{cm}$, indicating well-mixed, nearly flaw-free material, and thermal conductivities were about $1.10 \text{ W/cm}^\circ\text{C}$, which is relatively high for a near-isotropic graphite. Thermal expansion coefficients varied more widely than did most other properties, but were generally in the range 5.1 to $5.7 \times 10^{-6}/^\circ\text{C}$.

2. Effects of Thermax Additions: The graphites of Series 71, listed in Table III, were made from the same filler and binder used to manufacture the Series 65 graphites described above, but with additions of various amounts of Thermax carbon black to the raw mixes. Manufacturing procedures have been described in Report No. 14. It was found that additions of up to 15% Thermax to the filler had little effect on packed-filler or bulk density in the baked condition, but that bulk density after graphitizing increased with increasing Thermax concentration. However, Thermax additions of 10% or more caused radial cracking of the specimens to occur during the hot-molding operation. Because of this cracking, sound samples for tensile and compressive strength measurements could not be obtained from all of these graphites.

The properties of the Series 71 graphites are summarized in Table III, together with the properties of graphite 65B-1 which was prepared identically except that it contained no carbon black. Although the Thermax additions progressively increased bulk density, compressive strength, and Young's modulus, the increases were not large. A 5% Thermax addition reduced tensile strength, with little effect on flexure strength. However, larger additions also reduced flexure strength. Thermal expansion was apparently unaffected by the Thermax. Electrical resistivity was increased, and thermal conductivity was progressively reduced. All of these graphites were

nearly isotropic.

The desirability of a Thermax addition to this mix is evidently open to question, and depends upon the properties which are weighted most heavily. However, because of cracking during hot-molding, it is evident that no more than 5 to 10% of Thermax should be added to molded graphites of this type.

3. Resin-Bonded Graphites: Using Santa Maria filler Lot CP-17b, the molded graphites of Series 68 were made using furfuryl alcohol resins having low (250 cp), medium (1400 or 1600 cp), and high (9200 cp) viscosities. Two different concentrations of each binder were used: 20 and 25 pph. Manufacturing data are summarized in Report No. 14, and properties in Tables IV and V of this report. Many of the samples contained nearly random networks of very fine cracks, which undoubtedly affected the measured properties.

In the baked condition, both packed-filler and bulk density increased with molding pressure, as was the case for the pitch-bonded graphites discussed above. After graphitizing, however, the relation between bulk density and molding pressure varied with both binder viscosity and binder concentration. At 20 pph of binder, graphitized density increased with molding pressure for all binders. At 25 pph, however, this occurred only with the low-viscosity binder. With the medium-viscosity binder, graphitized density was nearly independent of molding pressure, and with the high-viscosity binder it decreased as molding pressure increased. Final densities were generally lower than those of the pitch-bonded graphites, principally because of less-dense packing of the filler.

On graphitizing, the resin-bonded materials shrank more than did their pitch-bonded counterparts, their shrinkage decreasing as molding pressure increased.

Some of the properties of these graphites are plotted in Fig. 4, 5, and 6. Most of the specimens were nearly isotropic, so that only with-grain properties are shown. Electrical resistivities, which are quite sensitive to the presence of flaws, were generally high but nearly isotropic, indicating that the crack pattern was nearly random. Presumably because of the cracks, none of the

TABLE IV

PROPERTIES OF RESIN-BONDED SANTA MARIA FILLER CP-17b WITH 20 PPH BINDER, SERIES 68A, B, C

SPECIMEN NO:	68A-1	68A-2	68A-3	68B-1	68B-2	68B-3	68C-1	68C-2	68C-3
Binder Viscosity, cp	250	250	250	1600	1600	1600	9200	9200	9200
Molding Pressure, psi	4000	1500	500	4000	1500	500	4000	1500	500
Density, g/cm ³	1.615	1.567	1.548	1.699	1.518	1.591	1.603	1.571	1.495
Tensile Str., psi									
With-grain	888	807	1192	2554	1240	1672	---	---	---
Compr. Str., psi									
With-grain	5046	3326	4921	10,196	5792	6586	---	---	---
Across-grain	5412	4588	5558	11,093	5982	6939	---	---	---
Flexure Str., psi									
With-grain	1425	1491	2004	3962	1874	2510	1693	2354	1456
Across-grain	1267	1646	2000	4109	2100	2636	2251	2574	1814
CTE x 10 ⁻⁶ /°C (a)									
With-grain	5.14	5.65	5.61	5.50	5.53	5.64	5.84	5.12	5.75
Across-grain	5.52	5.40	5.77	5.75	5.56	5.53	5.93	6.18	5.93
Resistivity, $\mu\Omega$ cm									
With-grain	1890	1894	2071	1523	1867	1940	1783	1844	2062
Across-grain	1883	1903	2077	1535	1869	1960	1878	1867	2096
Therm. Cond., W/cm°C									
With-grain	0.72	0.72	0.67	0.95	0.68	0.74	---	---	---
Across-grain	0.71	0.72	0.67	0.94	0.71	0.73	---	---	---
Young's Mod., 10 ⁶ psi									
With-grain	0.730	0.626	0.795	---	0.803	0.904	0.736	0.875	0.681
Across-grain	0.715	0.728	0.782	---	0.848	0.904	0.881	0.925	0.764
Anisotropies									
BAF ^(b)	1.009	1.009	~1.000	1.019	~1.000	~1.000	1.017	1.008	1.010
Compr. Str.	1.07	1.38	1.13	1.09	1.03	1.05	---	---	---
Flexure Str.	1.12	0.91	1.00	0.96	0.89	0.95	0.75	0.91	0.80
CTE	1.07	0.96	1.03	1.05	1.01	0.98	1.02	1.21	1.03
Resistivity	1.00	1.00	1.00	1.01	1.00	1.01	1.05	1.01	1.02
Therm. Cond.	1.01	1.00	1.00	1.01	0.96	1.01	---	---	---
Young's Mod.	1.02	0.86	1.02	---	0.95	1.00	0.84	0.95	0.89

(a) Coefficient of thermal expansion, average, 25-645°C.

(b) Bacon Anisotropy Factor, σ_{oz}/σ_{ox} .

properties of these graphites were as high as those of the pitch-bonded materials.

Young's modulus has not been plotted. Its trend with changing binder viscosity was very similar to that of flexure strength. At 20 pph of binder moduli were low, averaging about 0.8×10^6 psi. At 25 pph of binder

moduli ranged from 0.5 to 1.25×10^6 psi, and definitely increased with increasing binder viscosity.

At 20 pph of binder there is no clear trend of flexure strength with binder viscosity, although there is an indication that it may maximize at the intermediate viscosity. At 25 pph of binder, flexure strength tended to increase

TABLE V

PROPERTIES OF RESIN-BONDED SANTA MARIA FILLER CP-17b WITH 25 PPH BINDER, SERIES 68D, E, F

SPECIMEN NO.	68D-1	68D-2	68D-3	68E-1	68E-2	68E-3	68F-1	68F-2	68F-3
Binder Viscosity, cp	250	250	250	1400	1400	1400	9200	9200	9200
Molding Pressure, psi	4000	1500	500	4000	1500	500	4000	1500	500
Density, g/cm ³	1.599	1.522	1.446	1.683	1.703	1.701	1.686	1.713	1.741
Flexure Str., psi									
With-grain	1528	1020	1245	1768	2801	2714	2405	2257	3096
Across-grain	2170	1333	1293	2211	3343	3274	---	3149	2200
CTE x 10 ⁻⁶ /°C ^(a)									
With-grain	5.41	6.08	6.05	6.14	5.80	6.08	5.70	5.57	5.58
Across-grain	5.86	5.97	6.13	5.89	5.44	5.88	6.29	6.11	5.88
Resistivity, $\mu\Omega$ cm									
With-grain	2025	2129	2723	1742	1662	1649	1635	1554	1629
Across-grain	2114	---	2926	1791	1708	1648	1572	1820	1598
Young's Mod., 10 ⁶ psi									
With-grain	0.722	0.515	0.540	0.840	1.002	0.943	1.101	1.064	1.246
Across-grain	0.790	0.626	0.561	0.973	1.174	1.113	---	1.214	1.026
Anisotropies									
BAF ^(b)	1.019	~1.002	1.004	1.004	1.013	1.013	1.026	1.013	1.009
Flexure Str.	0.70	0.77	0.97	0.80	0.84	0.83	---	0.72	1.41
CTE	1.08	0.78	1.01	0.96	0.94	0.97	1.10	1.10	1.05
Resistivity	1.04	---	1.07	1.03	1.03	1.00	0.96	1.17	0.98
Young's Mod.	0.91	0.82	0.96	0.86	0.85	0.85	---	0.88	1.21

(a) Coefficient of thermal expansion, average, 25-645°C.

(b) Bacon Anisotropy Factor, σ_{oz}/σ_{ox} .

with viscosity. There is no clear correlation of flexure strength with molding pressure. In all cases, the flexure strengths of these resin-bonded graphites were low relative to those of the corresponding pitch-bonded samples.

Thermal expansion coefficients scattered quite broadly, and there were no obvious trends with either binder viscosity or molding pressure. The higher binder content gave a slightly higher expansion coefficient (about $5.8 \times 10^{-6}/^{\circ}\text{C}$ vs about $5.5 \times 10^{-6}/^{\circ}\text{C}$), which was also somewhat higher than that of the pitch-bonded graphites.

Electrical resistivity appeared to vary somewhat more systematically than did the other properties of the resin-bonded graphites. At 20 pph of binder resistivity decreased with increasing molding pressure, and appeared to minimize at the medium binder viscosity. At 25

pph resistivity decreased with increasing molding pressure in the case of the low-viscosity binder, but was nearly independent of both molding pressure and binder viscosity for the higher-viscosity binders. In general the higher binder concentration gave the lower resistivity values, but resistivities were considerably higher than for the pitch-bonded graphites.

Thermal shock indices for most of the resin-bonded Series 68 graphites were measured by C. R. King, LASL Group N-7. They are listed in Table VI and plotted as a function of bulk density in Fig. 6. Although these values are distinctly below the thermal shock value for commercial ATJ graphite, they are high for near-isotropic graphite, in spite of the crack structures of the samples.

Results for the 68E graphites, containing 25 pph of the

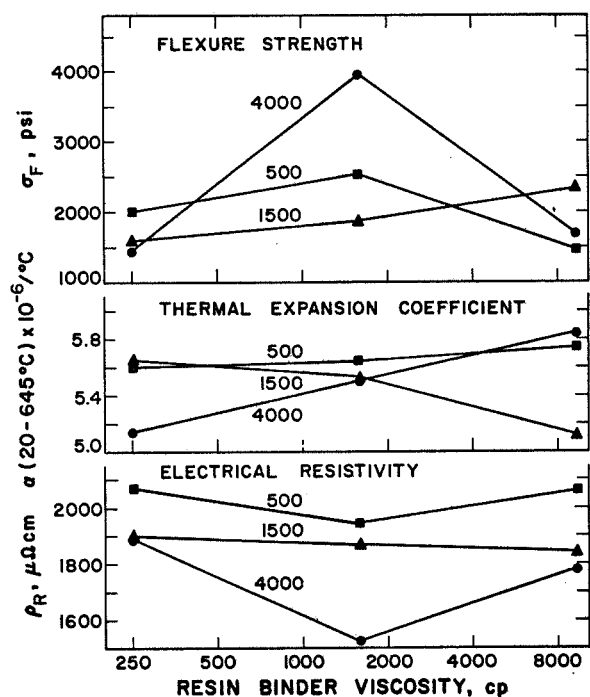


Fig. 4. The effect of binder viscosity on the with-grain properties of molded, resin-bonded Santa Maria graphites, Series 68, at a binder level of 20 pph, molded at 500, 1500, and 4000 psi.

medium-viscosity binder, are particularly encouraging. There are no obvious correlations of thermal shock resistance with the process variables considered in Table

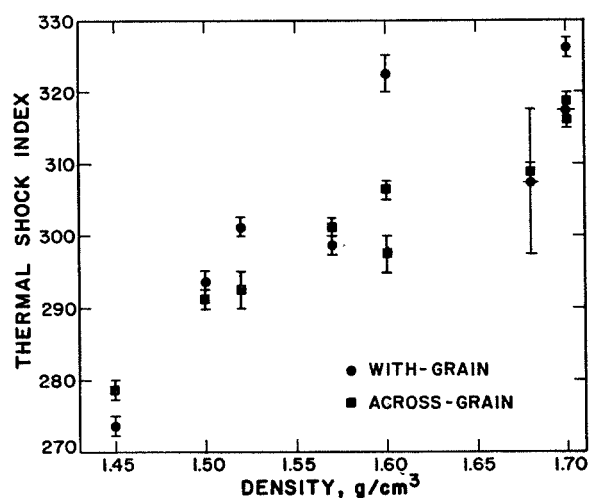


Fig. 6. The effect of bulk density on the thermal shock resistance of molded, resin-bonded, Santa Maria graphites.

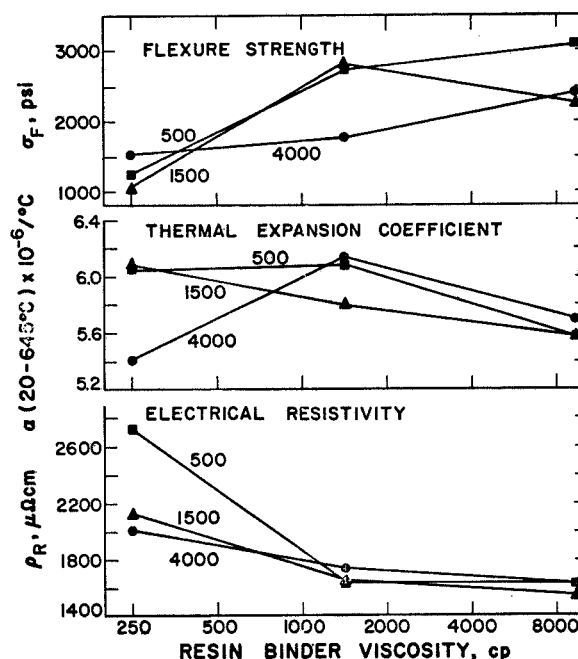


Fig. 5. The effect of binder viscosity on the with-grain properties of molded, resin-bonded graphites, Series 68, at a binder level of 25 pph, molded at 500, 1500, and 4000 psi.

VI, but Fig. 6 indicates a direct relation between thermal shock resistance and bulk density of the graphite.

Aside from the macroscopically visible cracks and the excessive porosity of these graphites, no gross defects were observed in them. The higher binder concentration (25 pph vs 20 pph) appeared to produce better mixing as well as increased binder residue. The medium and high viscosity binders appeared to yield better particle packing than did the low viscosity binder; however, mixing was relatively poor with the high viscosity binder. All specimens appeared to be deficient in fine particles less than about 50 μ dia. No overall optical anisotropy or preferred orientation of filler particles was observed microscopically.

D. Extruded Graphites (J. M. Dickinson)

Santa Maria fillers have also been used in investigations of experimental resin binders and of carbide additions, both of which are discussed in later sections of this report.

TABLE VI
THERMAL SHOCK INDICES OF SERIES 68 HOT-MOLDED RESIN-BONDED SANTA MARIA GRAPHITES

Sample	Binder		Molding Pressure, psi	Thermal Shock Index	
	Viscosity, cp	Conc. pph		WG	AG
ATJ (Control)	---	---	---	---	365/370
68C-1	9200	20	4000	320/325	295/300
68C-2	9200	20	1500	297.5/300	300/302.5
68C-3	9200	20	500	292.5/295	290/292.5
68D-1	250	25	4000	295/300	305/307.5
68D-2	250	25	1500	300/302.5	290/295
68D-3	250	25	500	272.5/275	277.5/280
68E-1	1400	25	4000	297.5/317.5	307.5/310
68E-2	1400	25	1500	325/327.5	315/317.5
68E-3	1400	25	500	315/320	317.5/320

III. HIGHLY ORIENTED POLYCRYSTALLINE GRAPHITES

A. Previous Work

Investigations of the production and properties of highly oriented graphites have previously been described in Reports No. 7, 8, 10, 11, 12, and 13 in this series.

Development of these graphites was undertaken in the hope that a combination of properties could be developed that would increase the resistance of graphite to ablative and other corrosive and erosive environments. In particular, high thermal conductivity is sought parallel to external surfaces to minimize hot spots, and low conductivity normal to those surfaces, to provide thermal insulation. Since this situation is favorable to development of high thermal stresses, high across-grain strength is also desired, to resist delamination. Other characteristics which would evidently be useful for ablation resistance are high density, fine filler-particle size, a tortuous void and grain-boundary structure, and a high degree of graphitization of both filler and binder residue.

Hot-molded graphites made from fine natural graphite fillers offer the possibility of meeting these requirements. Highly oriented structures are produced and, when the graphite is molded to a shape such as a hollow hemisphere or cone, most of the filler particles are oriented with their c-faces (which contain the high-

conductivity directions) nearly parallel to external surfaces. Unfortunately, such a graphite is very weak in the across-grain direction, normal to those surfaces. By adding a small proportion of Thermax carbon black to the filler, the across-grain strength can be significantly increased. Thus, a 5% Thermax addition yielded an oriented graphite with an across-grain flexure strength of above 1600 psi, accompanied by with-grain flexure strength of about 4800 psi. Larger Thermax additions progressively increased across-grain flexure strength, to about 2300 psi at 30% Thermax, with little effect on with-grain strength. However, the carbon black progressively reduced both with-grain thermal conductivity and the anisotropy of thermal conductivity. Thus, with no Thermax, with-grain and across-grain conductivities were 1.68 and 0.36 W/cm-°C respectively; with 30% Thermax they were 1.20 and 0.46 W/cm-°C.

B. Kynol Fiber Additions (R. J. Imprescia)

Two series of hot-molded graphites have been made using natural graphite fillers with additions of Kynol fiber instead of carbon black. Kynol is a phenolic fiber produced by the Carborundum Co., and was described in Report No. 12 in this series. It has a nominal diameter of 14 μ , and in this case was used at a cut length of about 0.25 in.

TABLE VII

MANUFACTURING DATA, HIGHLY ORIENTED GRAPHITES WITH KYNOL FIBER ADDITIONS

Specimen No.	Mix Composition, parts by weight			Calculated Binder Optimum, pph	Binder Residue ^(a) % (Baked)	Density, g/cm ³			Dimensional Change, Baked to Graphitized, %		
	Filler ^(b)	Binder				Packed Filler (Baked)	Bulk		$\Delta \ell$	Δd	Δv
		Kynol	30MH				Baked	Graph.			
75A-1b ^(c)	100.0	0	18	14.8	58.6	1.812	2.004	1.892	+2.4	+0.1	+2.7
75A-2	99.5	0.5	18	15.6	58.5	1.793	1.988	1.890	+1.8	+0.0	+1.9
75A-3	99.0	1.0	18	15.5	57.1	1.796	1.992	1.891	+1.8	+0.0	+1.9
75A-4	98.0	2.0	18	17.5	67.9	1.747	1.989	1.897	+1.6	0.0	+1.6
75A-5	96.0	4.0	18	18.3	68.4	1.729	1.999	1.904	+1.9	-0.0	+1.8
75B-1	100.0	0	14	10.0	42.3	1.939	2.054	1.903	+2.8	+0.3	+3.4
75B-2	99.5	0.5	14	12.3	58.1	1.876	2.035	1.892	+2.7	+0.2	+3.1
75B-3	99.0	1.0	14	13.9	57.7	1.834	2.037	1.892	+3.1	+0.1	+3.4
75B-4	98.0	2.0	14	12.4	58.6	1.868	2.047	1.891	+3.2	+0.1	+3.4
75B-5c	96.0	4.0	14	12.5	50.4	1.870	2.047	1.910	+2.9	+0.0	+3.0
75C-1	96.0	4.0	14	11.0	39.4	1.911	2.052	1.908	+2.4	+0.1	+2.6

(a) Binder residue includes Kynol Residue.

(b) Series 75A was made with filler G-21, and Series 75B and 75C with G-34.

(c) Specimen cracked circumferentially during graphitizing.

The graphites of Series 75A were made from the same fine natural graphite filler used for the experiments described above. This is Southwestern Graphite Co. Grade 1651, CMB-13 Lot G-21, and is all finer than 325 mesh. Series 75B graphites were made from a coarser natural graphite filler, Southwestern Graphite Co. Grade 1641, CMB-13 Lot G-34, which is about 68% minus 325 mesh. To each filler, Kynol fibers were added in concentrations of 0.5, 1.0, 2.0, and 4.0% by weight. Barrett 30MH coal-tar pitch was used in the proportions of 18 pph for the finer Lot G-21 filler and 14 pph for the coarser Lot G-34 filler. Standard solvent-blending and hot-mixing procedures were followed.

During the chopping step of the mixing operations (which involves extrusion through a food mill), it was necessary to reduce the rate at which the mix was fed to the mill as its Kynol content was increased, to avoid stalling the mill. Examination of the mixes after chopping revealed that a large proportion of the fibers had been reduced

in length. Several procedures were tried to avoid this, including increasing the discharge-plate hole size and removing the knife from the chopper head, but the reduction of fiber length still occurred. Specimen 75C-1 was made to determine the effect of avoiding this length reduction by omitting the chopping step. In this case vacuum mixing and drying were used instead, in a Ross Planetary Mixer, and there was no obvious breakage of fibers.

Hot-molding procedures ("Program A") were used to make specimens from all of these mixes. Graphitization was in flowing argon at about 2700°C except for specimen 75C-1, which was graphitized at only about 2600°C. Manufacturing data are given in Table VII.

For Series 75A, made with the finer natural graphite filler, packed filler density decreased as the Kynol fiber content increased, from 1.812 g/cm³ with no fiber to 1.729 g/cm³ at 4% Kynol. For the 75B series, made with the coarser filler, packed filler density was exceptionally high (1.939 g/cm³) with no fiber, decreased to a

TABLE VIII
PROPERTIES OF HIGHLY ORIENTED GRAPHITES MADE WITH KYNOL FIBER ADDITIONS

SPECIMEN NO:	Filler G-21					Filler G-34					
	75A-1b	75A-2	75A-3	75A-4	75A-5	75B-1	75B-2	75B-3	75B-4	75B-5c	75C-1
Kynol Fibers, %	0	0.5	1.0	2.0	4.0	0	0.5	1.0	2.0	4.0	4.0
Density, g/cm ³	1.892	1.890	1.891	1.897	1.904	1.903	1.892	1.892	1.891	1.910	1.908
Flexure Str., psi											
With-grain	4142	4347	4066	3513	4309	2044	2245	2386	2495	2678	3021
Across-grain	1600 ^(a)	1564	1473	1300	1484	652 ^(a)	701	675	641	673	678
Resistivity, $\mu\Omega$ cm											
With-grain	838	818	800	851	854	631	560	518	528	492	447
Across-grain	3608	3479	3363	3178	3624	1649	2257	3253	3582	3702	3561
Therm. Cond., W/cm ² °C											
With-grain	1.63	1.56	1.45	1.57	1.82	2.14	2.17	2.20	2.44	2.50	2.65
Across-grain	0.45	0.43	0.44	0.52	0.45	0.44	0.42	0.43	0.41	0.37	0.37
Anisotropies											
BAF ^(b)	3.10	2.54	2.57	2.62	2.95	2.78	2.41	3.34	3.44	3.64	3.573
M-Factor ^(c)	5.0	4.5	5.7	4.2	4.6	4.3	6.6	5.3	6.0	7.3	8.3
Flexure Str.	2.59	2.78	2.76	2.70	2.90	3.14	3.20	3.54	3.89	3.98	4.46
Resistivity	4.31	4.25	4.20	3.73	4.24	2.61	4.03	6.28	6.78	7.52	7.97
Therm. Cond.	3.62	3.63	3.30	3.02	4.04	4.86	5.17	5.12	5.95	6.76	7.16

(a) One test specimen only.

(b) Bacon Anisotropy Factor, σ_{OZ}/σ_{OX} .

(c) Exponent of cosine in cosine function which best represents angular distribution of intensities of reflected x-rays.

minimum value of 1.834 g/cm³ as Kynol content was increased to 1%, then increased with larger Kynol additions to 1.870 g/cm³ at 4% fiber. Specimen 75C-1, made without chopping, had high packed filler density (1.911 g/cm³) in spite of a Kynol addition of 4%.

Bulk densities in the baked condition were slightly higher for specimens made from the coarser filler, but were high for all specimens and showed no trend with changing Kynol content. All specimens increased significantly in volume during graphitization, the principal dimensional change being an increase in axial length (i.e., expansion in the across-grain direction). Graphitized densities were in the range 1.89 to 1.91 g/cm³ for all specimens, and showed no trend with Kynol concentration and no significant difference for the two fillers. During graphitization, Specimen 75A-1b developed a hairline crack on its cylindrical surface perpendicular to the molding axis.

Other properties of these graphites are listed in Table VIII and plotted in Fig. 7 and 8. The Series 75A graphites, made from the finer (G-21) filler were essentially unaffected by the Kynol additions, although reduced specimen breakage during machining indicated that the Kynol had a useful effect. The Series 75B graphites, made from the coarser (G-34) filler, had higher anisotropies and lower flexure strengths than did specimens made from the finer natural graphite. With-grain strength and thermal conductivity, across-grain electrical resistivity, and all measures of anisotropy increased with Kynol concentration. With-grain thermal conductivity was initially quite high (2.1 W/cm²°C) and increased continuously to 2.5 W/cm²°C at 4% Kynol, while across-grain conductivity decreased from 0.42 to 0.37 W/cm²°C as Kynol concentration increased from 0 to 4%.

The strengths of all of these graphites were low compared with those of graphites made with Thermax instead

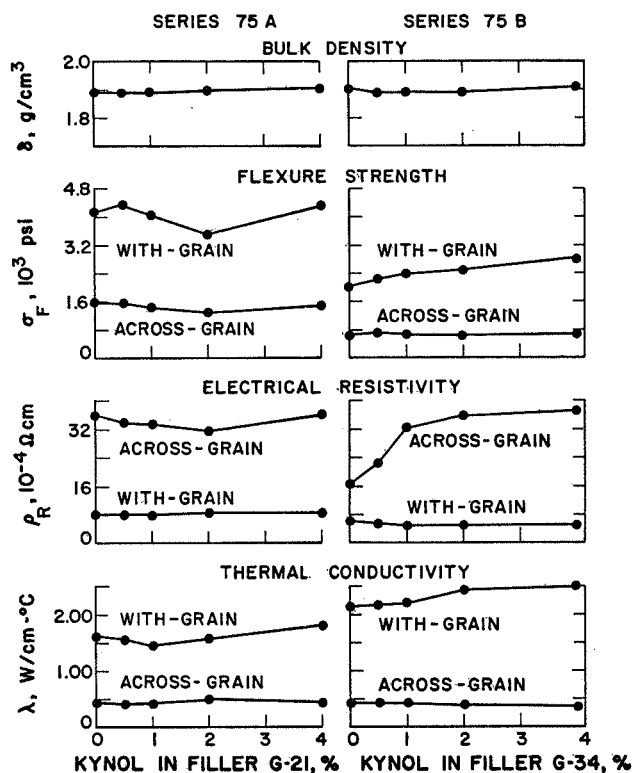


Fig. 7. Effects of Kynol fiber additions on the properties of graphites made from two natural graphite fillers.

of Kynol additions. The effect of the Kynol on both with-grain and across-grain thermal conductivity is encouraging, especially in the case of the coarser natural graphite filler. Since Thermax additions increase strength and reduce with-grain conductivity, a combination of Thermax and Kynol will be tried, in the hope that a strengthening effect will be produced by the Thermax and the thermal conductivity maintained by the Kynol.

Specimen 75C-1, in whose preparation the chopping step was omitted, had properties similar to those of specimen 75B-5c, but had slightly higher anisotropies. Apparently fiber breakage was at least reduced by using a planetary mixer instead of a food chopper, with no sacrifice of properties.

C. Needle-Coke Graphites (R. J. Imprescia)

Needle cokes grind to highly acicular particles which are easily oriented by the shearing forces developed in a forming operation. They are, therefore, also candidate

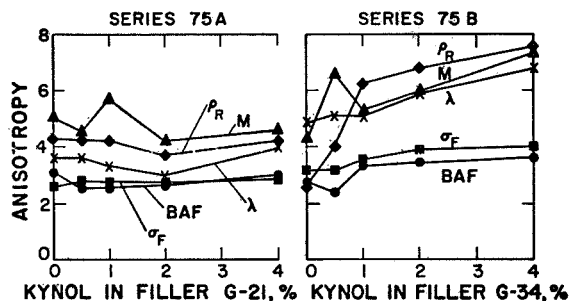


Fig. 8. Effects of Kynol fiber additions on the anisotropies of graphites made from two natural graphite fillers.

filler materials for the manufacture of highly oriented graphites, and in general have the advantage of higher chemical purity than a natural graphite. Accordingly, an investigation has been undertaken of the usefulness of a needle coke in this application. The particular coke being studied is Union Carbide Corporation's Needle Coke No. 1, CMB-13 Lot CNL-1. In order to compare the grinding characteristics of cokes having widely different internal structures, preparation of the needle-coke fillers was essentially identical with that of the series of Santa Maria fillers described in Report No. 11.

The lump needle coke was screened through 1/2-in. hardware cloth, which has openings nominally 29/64-in. square, and minus 8-mesh undersize was screened out and discarded. Six small lots of the plus 8-mesh lump coke were then heat-treated at the temperatures listed in Table IX, which ranged from 1230 to 2715°C. These and a sample in the as-received condition (calcined by the manufacturer at a temperature estimated to be 1190°C) were then ground by the standard "S+T+I" procedure, involving two stages of hammer milling and one of fluid-energy milling. The particle characteristics of the grinding products were determined by x-ray diffraction, sedimentation analysis, surface-area analysis, and helium pycnometry. Crystalline parameters (d_{002} and L_c) have been discussed in Report No. 14 in this series. Helium densities, particle-size statistics, and surface-area data are listed in Table IX of this report. Surface areas and grindabilities calculated from them are listed

TABLE IX
PARTICLE CHARACTERISTICS OF NEEDLE COKE GRINDING PRODUCTS

	Screened Feed ^(a)	Pre-Grind Heat-Treatment Temperature, °C						
		1190 ^(b)	1230	1520	1825	2130	2420	2715
Helium Density, δ_{He} , g/cm ³	---	2.133	2.166	2.170	2.163 ^(c)	2.176	2.199	2.207
Micromerograph Sample Statistics ^(d)								
\bar{x}_3	8.328	1.555	1.704	1.644	1.825	2.133	2.338	2.104
s_x^2	2.772	0.162	0.294	0.333	0.286	0.264	0.242	0.274
\bar{x}	6.718	-0.271	-0.029	0.009	-0.139	0.270	0.494	0.256
\bar{d}_3 , microns	4955	6.113	6.769	6.212	7.654	11.184	14.450	12.417
\bar{d} , microns	2233	0.868	1.187	1.256	1.071	1.579	1.944	1.561
s_d^2 , microns ²	801,600	0.481	1.083	1.215	1.068	1.924	2.663	1.768
S_W , cm ² /g	7.0	8535	6576	6695	5979	4539	3799	4773
CV_d	0.60	0.799	0.877	0.878	0.964	0.878	0.839	0.852
BET Surface Area Data								
S_W , m ² /g	---	27.744	24.873	27.128	14.980	10.007	9.274	10.502
d_s ^(e)	---	0.101	0.111	0.102	0.185	0.276	0.294	0.259
Fuzziness Ratio ^(f)	---	32.51	37.82	40.52	25.05	22.05	24.41	22.00

(a) Particle-size data for screened feed material is based on sieve analysis.

(b) Estimated temperature at which feed material was calcined by manufacturer.

(c) Average of 9 determinations on 2 samples.

(d) Finite interval calculation.

(e) $d_s = 6/\delta_{\text{He}} S_W$

(f) Ratio of measured (BET) surface area to that calculated from Micromerograph data.

in Table X, where they are compared with similar data for Santa Maria coke.

Particle-size distribution curves for these grinding products are plotted in Fig. 9. In general as the pre-grind heat-treatment temperature was increased the distribution became more nearly lognormal. The data of Table IX indicate that as heat-treatment temperature was increased to 2420°C grinding became more difficult; both weight-average (\bar{d}_3) and number-average (\bar{d}) particle-size increased and both calculated and measured (BET) surface area decreased. Above 2420°C these trends were reversed and grindability increased. The curves of Fig. 9 are in agreement with these data, although the

curve representing material graphitized at 2715°C before grinding is anomalous in showing a sharp change in slope at a particle size of about 20 μ .

Grindability, defined as the rate of generation of new surface during grinding, was determined for each grinding product from the surface area calculated from Micromerograph sample statistics. (Surface area measured by the BET method includes surface-connected internal porosity, and therefore a large increment of area which was not created by grinding.) Surface areas and grindabilities of the needle coke are compared in Table X and Fig. 10 with those of Santa Maria coke in similar conditions of heat-treatment. After heat-treatment at any

TABLE X
SURFACE AREAS AND GRINDABILITIES OF NEEDLE AND SANTA MARIA COKES

Coke	Heat-Treat Temp., °C	Surface Area, m ² /g ^(a)		Grindability, m ² /min ^(c)
		S _W	ΔS _W ^(b)	
Santa Maria	Green ^(d)	0.0009	0.0000	---
	620	0.876	0.875	13.1
	900	0.607	0.606	9.1
	1215	0.453	0.452	6.4
	1515	0.372	0.371	5.6
	1833	0.280	0.279	4.2
	2147	0.227	0.226	3.4
	2468	0.266	0.265	4.0
	2808	0.303	0.302	4.5
	Feed ^(d)	0.0007	0.0000	---
Needle	1190 ^(e)	0.854	0.853	12.9
	1230	0.658	0.657	9.9
	1520	0.669	0.658	10.0
	1825	0.598	0.597	8.9
	2130	0.454	0.453	6.8
	2420	0.380	0.379	5.7
	2715	0.477	0.476	7.1

(a) Calculated from Micromerograph data.

(b) New Surface generated by grinding.

(c) New surface generated per minute at feed rate to the mill of 15 g/min.

(d) Screened feed material before grinding.

(e) Estimated calcining temperature used by manufacturer.

given temperature the grindability of the needle coke is considerably higher than that of the Santa Maria coke. However, for both cokes, grindability decreases rapidly as calcining temperature increases, passes through a minimum, and then increases as significant graphitization occurs. For Santa Maria coke the minimum occurred at about 2200°C, for the needle coke at about 2400°C.

Hot-molded graphites (Series 69) were made from the individual needle-coke grinding products listed in Table IX. These fillers were mixed with Barrett 30MH coal-tar pitch using standard solvent-blending methods, then hot-molded using "Program A." Binder requirements were determined in preliminary runs in which

large excesses of pitch were used, and were found to vary greatly with pre-grind heat-treatment temperature. All specimens were graphitized in flowing argon to about 2800°C. Manufacturing and density data are summarized in Table XI. Properties of the graphitized specimens are listed in Table XII and plotted as functions of filler heat-treatment temperature in Fig. 11 and 12.

With these fillers there was no apparent correlation between coefficient of variation of the particle-size distribution (CV_d) and packing efficiency. Packing efficiency and bulk density did, however, increase with pre-grind heat-treatment temperature, and densities after graphitization were very high for fillers that had been heat-treated at and above 1825°C. Using a flaky filler and a

TABLE XI
MANUFACTURING DATA, HOT-MOLDED, PITCH-BONDED, NEEDLE-COKE GRAPHITES, SERIES 69

Specimen No.	Filler Heat-Treat Temp. °C	Binder Conc. pph	Calculated Binder Optimum, pph	Binder Residue, % (Baked)	Packed Filler Density, g/cm ³	Packing Efficiency, ^(a) %	Bulk Density, g/cm ³		Dimensional Change, Baked to Graphitized, %		
							Baked	Graph.	Δl	Δd	Δv
69D-1	1190	32	30.7	62.6	1.439	67.5	1.727	1.782	-3.5	-0.5	-4.5
69E-1	1230	31	28.5	64.1	1.480	68.3	1.774	1.812	-2.6	-0.4	-3.3
69F-1	1520	28	27.4	68.4	1.500	69.1	1.788	1.827	-2.4	-0.4	-3.2
69G-1	1825	28	19.8	56.3	1.637	75.7	1.877	1.899	-1.0	-0.0	-1.8
69H-1 ^(b)	2130	23	19.1	66.9	1.658	76.2	1.914	1.912	-0.2	-0.1	-0.4
69I-1	2420	21	20.3	72.0	1.646	74.9	1.895	1.906	-1.1	0.0	-1.0
69J-1	2715	18	16.6	71.0	1.731	78.4	1.952	1.929	+0.9	0.0	+0.9

(a) Packing Efficiency = (Packed Filler Density)/(Helium Density of Filler).

(b) Maximum molding temperature was 820°C.

forming method that encourages parallel stacking of such particles, it is probable that packing is influenced more by the distribution of particle shapes than by the distribution of sizes. The higher degree of graphitization and the better-developed cleavage produced by a higher temperature heat-treatment of the coke favor grinding to flakes of relatively uniform thickness, which stack more efficiently

than do less-regular shapes. However, other factors are also involved in particle packing. One is the increased

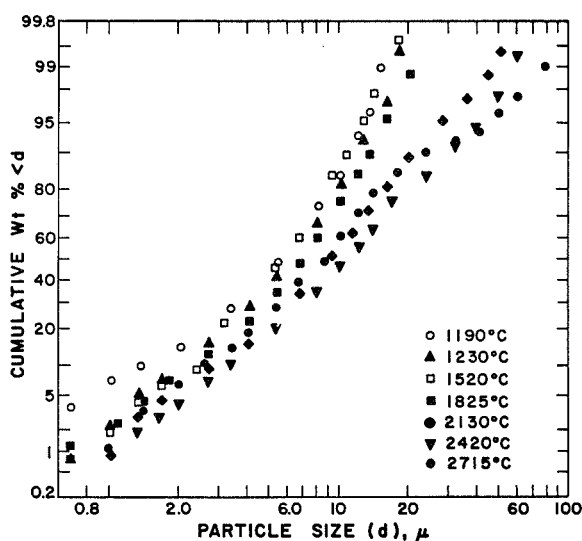


Fig. 9. Micromerograph particle-size data for needle coke heat-treated at the indicated temperatures then ground by the standard "S+T+I" procedure.

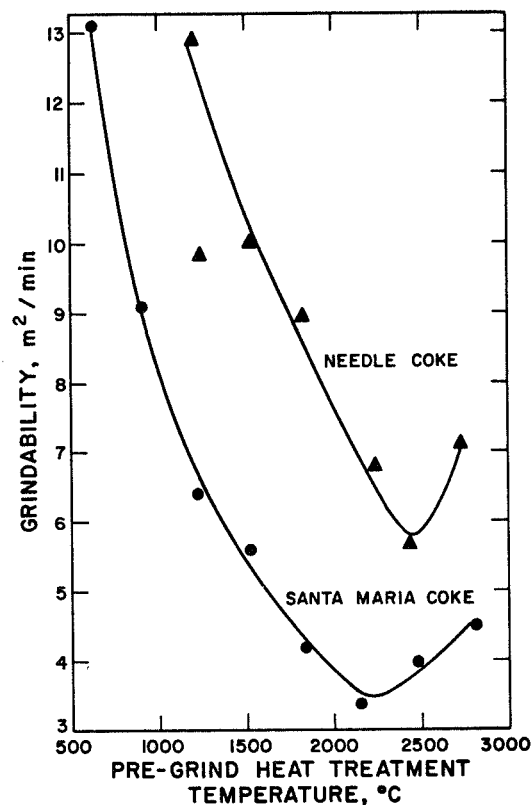


Fig. 10. Grindability as a function of pre-grind heat-treatment temperature for Santa Maria and needle cokes.

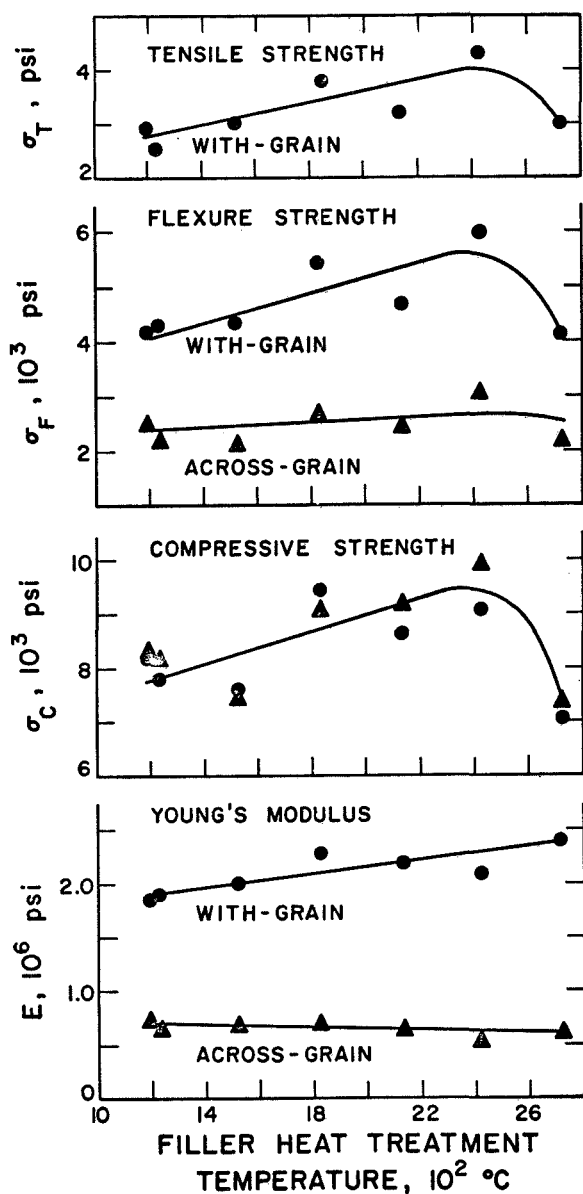


Fig. 11. Effects of pre-grind filler heat-treatment temperature on the mechanical properties of needle-coke graphites, Series 69.

flexibility of a more highly graphitic flake, which permits it to accommodate better to stacking irregularities. Another is the tendency of particles to form clumps. It was observed microscopically that fillers which had been heat-treated only to 1825°C or less were grouped into clumps up to about 1 mm in their maximum dimensions, which had been flattened by the molding process. Within a clump the filler flakes were generally parallel, but there were often large misorientations between clumps. This

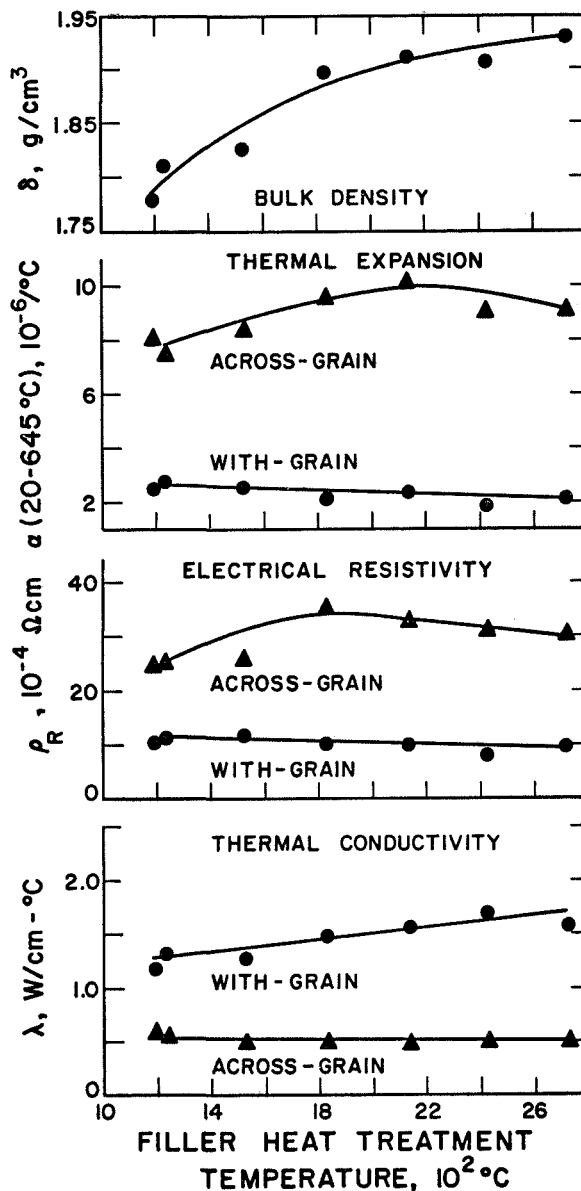


Fig. 12. Effects of pre-grind filler heat-treatment temperature on the physical properties of needle-coke graphites, Series 69.

probably affected both density and anisotropy, and may have had a larger effect on other properties. All samples which contained clumps also contained cracks within the clumps. The cracks were parallel to the long dimensions of the filler flakes, and in general did not propagate beyond the clump. When the pre-grind filler heat-treatment had been to 2420°C or higher there was very little clumping, a higher degree of preferred orientation, and no detectable cracks.

TABLE XII
PROPERTIES OF HOT-MOLDED NEEDLE-COKE GRAPHITES, SERIES 69

SPECIMEN NO:	69D-1	69E-1	69F-1	69G-1	69H-1	69I-2	69J-1
Filler HTT ^(a) , °C	1190	1230	1520	1825	2130	2420	2715
Density, g/cm ³	1.782	1.812	1.827	1.899	1.912	1.906	1.929
Tensile Str., psi							
With-grain	2972	2554	3013	3800	3210	4320	2999
Compr. Str., psi							
With-grain	8200	7809	7605	9459	8646	9076	7076
Across-grain	8298	8170	7447	9077	9190	9914	7347
Flexure Str., psi							
With-grain	4248	4325	4389	5543	4697	6007	4128
Across-grain	2472	2172	2114	2699	2413	3038	2192
CTE, $\times 10^{-6}/^{\circ}\text{C}$ ^(b)							
With-grain	2.56	2.78	2.59	2.19	2.44	1.90	2.18
Across-grain	8.10	7.50	8.42	9.49	10.10	9.03	9.27
Resistivity, $\mu\Omega$ cm							
With-grain	1081	1133	1176	1033	1011	834	990
Across-grain	2449	2534	2581	3507	3279	3109	3042
Therm. Cond., W/cm-°C							
With-grain	1.19	1.33	1.28	1.49	1.58	1.71	1.60
Across-grain	0.59	0.54	0.52	0.51	0.49	0.52	0.51
Young's Mod., 10^6 psi							
With-grain	1.866	1.905	2.023	2.281	2.192	2.090	2.410
Across-grain	0.725	0.651	0.685	0.690	0.642	0.544	0.615
Anisotropies							
BAF ^(c)	1.805	1.951	1.957	2.466	2.130	2.327	2.429
M-Factor ^(d)	2.64	2.96	2.71	3.26	3.10	3.37	3.98
Compr. Str.	1.01	1.05	0.98	0.96	1.06	1.09	1.04
Flexure Str.	1.72	1.99	2.08	2.05	1.95	1.98	1.88
CTE	3.16	2.70	3.25	4.33	4.14	4.75	4.25
Resistivity	2.27	2.24	2.19	3.39	3.24	3.73	3.07
Therm. Cond.	2.01	2.46	2.46	2.92	3.22	3.29	3.14
Young's Mod.	2.57	3.10	2.95	3.31	3.41	3.84	3.92

(a) Filler Heat Treatment Temperature.

(b) Coefficient of Thermal Expansion, average, 25-645°C.

(c) Bacon Anisotropy Factor, σ_{oz}/σ_{ox} .

(d) Exponent of cosine in cosine function which best represents angular distribution of intensities of reflected x-rays.

Tensile, flexure, and compressive strengths of these graphites increased with filler heat-treatment temperature to about 2400°C, and then appeared to fall off--although data scatter was such that it is not clear that there are maxima at 2400°C in the curves of Fig. 11.

Strength values were encouraging, especially the across-grain flexure strength of about 3000 psi for sample 69I-2, made from a filler heat-treated at 2420°C. In the with-grain direction, Young's modulus increased almost linearly with filler heat-treatment temperature, to a

TABLE XIII
MOLECULAR DISTRIBUTIONS OF SEVERAL FURFURYL ALCOHOL RESINS

Binder Identification	Viscosity, cp	Proportion of Resin in Each Distribution Region, %				Sample Statistics				Coefficient of Variation
		1	2	3	4	Mean	Variance	Deviation	Skewness	
Varcum 8251	200	27.4	24.5	27.4	20.7	2.41	1.22	1.10	0.09	0.46
QX 247	880	15.2	33.9	35.5	15.4	2.51	0.87	0.93	-0.02	0.37
EMW 305	960	10.8	39.3	38.9	11.1	2.50	0.69	0.83	0.004	0.33
EMW 1400	1400	11.3	37.7	39.4	11.6	2.51	0.71	0.85	-0.02	0.34
EMW 260	1475	11.4	38.1	39.9	10.6	2.50	0.70	0.83	-0.02	0.33
EMW 1600	1600	9.5	38.6	40.8	11.2	2.54	0.67	0.82	-0.01	0.32
QX 248	2000	12.5	34.3	37.4	15.9	2.57	0.82	0.91	-0.04	0.35
EMW 304	2050	9.0	37.4	42.1	11.5	2.56	0.66	0.81	-0.03	0.32

maximum value of 2.4×10^6 psi. In the across-grain direction it decreased slightly.

Both thermal expansion coefficient and electrical resistivity appeared to maximize for the with-grain orientation at a filler heat-treatment temperature near 2000°C, and for the across-grain orientation to decrease continuously as heat-treating temperature increased. Thermal conductivity in the with-grain direction increased continuously with filler heat-treatment temperature, to the relatively high value of about 1.7 W/cm-°C. In the across-grain direction it remained nearly constant at about 0.5 W/cm-°C.

Although anisotropies were distinctly less than those of similar graphites made from natural graphite fillers, they were relatively high and in general increased with filler heat-treatment temperature up to at least 2420°C.

The highest with-grain thermal conductivity (1.7 W/cm-°C) in this series closely approaches the highest value (1.8 W/cm-°C) so far measured for an oriented graphite made with a fine natural graphite filler (Lot G-21). The highest across-grain flexure strength (3038 psi) was measured on the same graphite--Specimen 69I-2--that had the highest conductivity, and was nearly twice the highest across-grain strength so far observed when a natural graphite filler was used. Obviously, a highly oriented graphite made from a properly heat-treated and ground needle coke may be very interesting for applications of the type here being considered.

Further experiments are planned in which finely ground needle cokes will be used both as the principal fillers and as additives to other fillers such as natural graphites.

IV. GRAPHITE-CARBIDE COMPOSITES

A. Previous Work

Investigations of the production and properties of graphites modified by additions of ZrC particles have previously been described in Reports No. 14 and 15 in this series.

B. Extruded Graphite and Composite Tubes (J. M. Dickinson)

The graphite-ZrC composites previously investigated were made using either Varcum 8251 or EMW 1400 furfural alcohol resin binder. The investigations have now been extended to include four other furfuryl alcohol resin binders. All of these binders are described in Table XIII by means of a system described in Report No. 8, in which the gel-permeation chromatogram of the resin is arbitrarily subdivided into four sequentially numbered regions representing fractions having progressively larger mean molecular sizes. Varcum 8251 is a commercial resin produced by the Varcum Chemical Division of Reichold Chemicals, Inc. The two "QX" binders are

TABLE XIV
MANUFACTURING CONDITIONS, ACV GRAPHITE TUBES

Specimen Number	Extrusion Section	Binder Used	Extrusion Conditions				
			Pressure, psi	Velocity, in./min	Vacuum, Torr	Temperature, °C	
ACV 1	1	Varcum 8251	8100	171	< 1000	41	46
	2		9000	200	< 1000	41	46
	3		13500	900	600	41	46
	4		7425	97	600	41	46
ACV 2	1	Varcum 8251	10125	164	450	41	50
	2		14125	450	450	41	50
	3		15975	800	450	41	50
	4		11425	120	450	41	50
ACV 3	1	EMW 1400	20000	257	500	45	50
	2		22050	257	500	45	50
	3		22050	257	500	45	50
ACV 4	1	Varcum 8251	10575	360	500	49	48
	2		9450	138	500	49	48
	3		10350	267	500	49	48
	4		9225	32	500	49	48
ACV 5	1	Varcum 8251	13275	225	1000	42	47
	2		15400	277	1000	42	47
	3		17100	720	1000	42	47
	4		13050	68	1000	42	47
ACV 6	1	QX 247	21775	150	475	40	48
	2		22725	78	475	40	48
ACV 7	1 (a)	QX 248	22725	319	475	47	46
ACV 8 ^(b)	1 (a)	QX 247	22725	64	500	52	48
	2		22725	64	500	52	48
	3		22725	64	500	52	48

(a) Very fine surface cracks.

(b) All sections extruded without stopping press.

experimental resins made by the Quaker Oats Co. The "EMW" binders were synthesized in CMB-13.

To evaluate the effects of the carbide additions as well as those of the various binders, the ACV series of graphites was made with no carbide added. The ACW series of composites was then made with the same fillers and binders, but enough ZrC was added so that the graphitized products would contain 30 vol % ZrC.

Manufacturing conditions for the two series are listed in Tables XIV and XV.

Graphites ACV1 and ACV4 were made from a mix containing 85 parts of Great Lakes Grade 1008-S graphite flour (CMB-13 Lot G-18) and 15 parts of Thermax carbon black. In all other graphites and in all composites, the principal filler was Santa Maria graphite flour, CMB-13 Lot G-26 (Y-12 "Blend 1"). In general the

TABLE XV
MANUFACTURING CONDITIONS, GRAPHITE-ZrC COMPOSITE TUBES

Specimen Number	Extrusion Section	Binder ^(a) Used	Extrusion Conditions				
			Pressure, psi	Velocity, in./min	Vacuum, Torr	Temperature, °C	
ACW 1	1	EMW 1400	19260	200	600	45	49
	2		18630	171	600	45	49
	3		19260	189	600	45	49
	4		21960	289	600	45	49
	5		14440	48	600	45	49
ACW 2	1	Varcum 8251	10080	300	600	45	50
	2		9450	150	600	45	50
	3		9990	240	600	45	50
	4		12150	900	600	45	50
	5		8280	57	600	45	50
ACW 3	1	QX 247	20475	180	400	50	50
	2		22050	277	400	50	50
	3		17685	92	400	50	50
	4		20025	200	400	50	50
ACW 4 ^(b)	1	QX 248	22500	95	400	60	50
	2		22500	28	400	60	50
	3		22500	<10	400	60	50
ACW 5	1	EMW 305	22825	84	550	44	48
	2		22825	47	550	44	48
	3		22825	56	550	44	48
	4		22825	67	550	44	48
ACW 6	1	EMW 304	21750	200	400	46	50
	2		21100	144	400	46	50
	3		21150	133	400	46	50
	4		21150	124	400	46	50

(a) 13.9 pph binder used for all specimens.

(b) Mix was very dry.

extrusions were made in sections about 8 ft long, and the press was stopped between sections. As is indicated in Tables XIV and XV, extrusion speed and pressure were usually changed from one section to the next. However, graphite ACV8 was made without stopping the press between sections. All extrusions were tubes 0.25 in. O.D. and 0.1 in. I.D. Curing, baking, and graphitizing cycles were normal for resin-bonded graphites.

Because of the rather large differences in pressure and speed used in extruding different sections of the same extrusion batch, the properties of the finished tubes have been tabulated in two ways. In Tables XVI and XVII, the properties of all extrusion sections are listed. In Table XVIII "selected average" values are given, representing average values from runs which were not made under unusual conditions. Only with-grain properties are listed.

TABLE XVI
PROPERTIES OF ACV GRAPHITE TUBES

Specimen Number	Extrusion Section	Binder Used	Bulk Density, g/cm ³	Binder Carbon Residue, %	Young's Modulus, 10 ⁶ psi	Electrical Resistivity, $\mu\Omega$ cm	CTE, (a) $\times 10^{-6}/^{\circ}\text{C}$
ACV 1	1	Varcum 8251	1.803	36.6	2.09	1309	2.17
	2		1.810	37.4	2.11	1301	
	3		1.822	38.2	2.17	1278	
	4		1.789	36.9	2.06	1333	
ACV 2	1	Varcum 8251	1.792	37.7	1.35	1934	4.61
	2		1.768	38.0	1.31	1979	
	3		1.788	36.9	1.37	1972	
	4		1.780	36.1	1.29	2042	
ACV 3	1	EMW 1400	---	---	1.55	1832	4.75
	2		1.832	---	1.48	1911	
	3		---	---	1.47	1911	
ACV 4	1	Varcum 8251	1.803	38.1	2.08	1363	
	2		1.804	38.6	2.04	1386	
	3		1.813	39.0	2.14	1362	
	4		1.867	39.0	2.06	1382	
ACV 5	1	Varcum 8251	1.797	39.0	1.42	1986	
	2		1.771	38.8	1.37	2031	
	3		1.774	38.7	1.37	2018	
	4		1.768	37.8	---	2014	
ACV 6	1	QX 247	1.768	36.7	1.29	---	
	2		1.781	37.2	1.25	---	
ACV 7	1	QX 248	1.789	38.1	1.36	2014	
ACV 8	1	QX 247	1.811	41.3	1.43	1852	
	2		1.818	40.4	1.39	1919	
	3		1.802	39.3	1.32	1985	

(a) Coefficient of thermal expansion, average, 25-645°C.

The densities of both the ACV graphites and the ACW composites in general increased with extrusion pressure. Otherwise the properties of both types of material varied rather unsystematically with extrusion conditions. Apparently, however, either very high or very low extrusion speeds are undesirable.

The graphites of the ACV series are very much inferior to graphites previously made as extruded 0.5-in. dia rods from similar raw mixes. At least in part this is

because of the tubular geometry of the ACV extrusions, as is discussed in a later section of this report. It may also be due in part to die design and to the high reduction ratio and extrusion pressures used. The low densities of these graphites appear to result from a network of connected porosity, often appearing as joined small cracks. Many microcracks up to 200 μ long were observed. The effects of porosity and microcracks overshadowed any effects of changing binders.

TABLE XVII
PROPERTIES OF GRAPHITE-30 v/o ZrC TUBES, SERIES ACW

Specimen Number	Extrusion Section	Binder Used	Bulk Density, g/cm ³	Binder Carbon Residue, %	Young's Modulus, 10 ⁶ psi	Electrical Resistivity, $\mu\Omega$ cm	CTE ^(a) x 10 ⁻⁶ /°C	Strengths		
								Flexure, psi	Tensile, psi	Compressive, psi
ACW 1	1 ^(b)	EMW 1400	3.151	38.3	5.33	233	6.51 ^(c)	---	---	---
	2		3.159	37.9	5.43	223	---	13500	---	28000
	3		3.160	36.5	5.34	231	---	---	---	---
	4			36.1	5.40	230	---	---	---	---
	5		3.168	36.8	5.42	233	---	13000	---	---
ACW 2	1	Varcum 8251	3.087	33.2	4.87	---	---	---	---	---
	2		3.075	32.8	4.83	234	5.50 ^(d)	---	---	24000
	3		3.091	33.2	4.88	231	---	12500	---	---
	4		3.072	33.5	4.80	224	---	12500	6000	---
	5		3.081	33.8	4.82	245				
ACW 3	1	QX 247	3.153	---	5.68	197				
	2		3.162	---	5.56	198				
	3		3.156	---	5.75	199				
	4		3.151	---	5.75	203				
ACW 4	1	QX 248	3.194	38.4	5.92	193				
	2		3.191	38.4	5.86	194				
	3		3.162	36.7	5.55	192				
ACW 5	1	EMW 305	3.146	38.2	5.35	234				
	2		3.137	38.1	5.32	240				
	3		3.158	37.8	5.33	245				
	4		3.146	37.7	5.40	240				
ACW 6	1	EMW 304	3.166	38.1	5.37	256				
	2		3.170	38.1	5.32	259				
	3		3.169	38.8	5.35	252				
	4		3.168	38.9	5.36	249				

(a) Coefficient of thermal expansion, average, 25-645°C.

(b) Slow heat-treatment.

(c) Across-grain CTE = 5.98×10^{-6} /°C.

(d) Across-grain CTE = 5.95×10^{-6} /°C.

This was not true of the composites of the ACW series. It is not clear that the specimen geometry and extrusion conditions were such that composites of the highest possible quality were produced. In general, however, densities were quite high and properties were good. Both density and strength were higher when Varcum 8251 was

replaced with a binder having higher viscosity and a narrow molecular size distribution. The two experimental Quaker Oats resins performed well in this series; however, a better evaluation of them is presented in the "Raw Materials" section of this report.

TABLE XVIII
PROPERTIES OF SELECTED ACW GRAPHITE-30 v/o ZrC AND ACV GRAPHITE TUBES

Specimen Number	Binder Used	Bulk Density, g/cm ³	Binder Carbon Residue, %	Young's Modulus, 10 ⁶ psi	Electrical Resistivity, $\mu\Omega$ cm	CTE ^(a) , $\times 10^{-6}/^{\circ}\text{C}$	ZrC Content, Vol. %	Strengths		
								Flexure, psi	Tensile, psi	Compressive, psi
ACW 1	EMW 1400	3.160	37.1	5.38	209	6.51 ^(b)	30	13500	---	28000
ACW 2	Varcum 8251	3.083	33.1	4.84	234	5.50 ^(c)	30	12600	6100	24000
ACW 3	QX 247	3.156	37.2	5.60	199	---	30			
ACW 4	QX 248	3.182	37.8	5.78	193	---	30			
ACW 5	EMW 305	3.147	37.9	5.35	240	---	30			
ACW 6	EMW 304	3.168	38.5	5.34	250	---	30			
ACV 1	Varcum 8251	1.806	37.3	2.11	1303	2.17	0			
ACV 2	Varcum 8251	1.782	37.2	1.33	1982	4.61	0			
ACV 3	EMW 1400	1.832	---	1.50	1885	4.75	0			
ACV 4	Varcum 8251	1.807	38.6	2.08	1373	---	0			
ACV 5	Varcum 8251	1.778	38.6	1.38	2012	---	0			
ACV 6	QX 247	1.775	37.0	1.27	---	---	0			
ACV 7	QX 248	1.789	38.1	1.36	2014	---	0			
ACV 8	QX 247	1.810	40.5	1.38	1909	---	0			

(a) Coefficient of thermal expansion, average, 25-645°C.

(b) Across-grain CTE = $5.98 \times 10^{-6}/^{\circ}\text{C}$.

(c) Across-grain CTE = $5.95 \times 10^{-6}/^{\circ}\text{C}$.

The relatively high quality of the ACW composites as compared with the ACV graphites is probably due largely to an improvement in packing behavior which occurs when this particular zirconium carbide powder (Lot ZrC-77-D) is added to the Lot G-26 graphite flour filler. (This was discussed in Report No. 15, pp 23-25.) The formation of relatively large quantities of reorganized graphite around the ZrC particles during the graphitizing heat treatment may also be important, since this forms primarily at the expense of the binder residue, which contains most of the normal defects of the graphite structure.

V. RAW MATERIALS

A. Filler Flours (H. D. Lewis)

Samples of four different filler flours have been obtained from LASL Group CMB-6 and characterized. These were: Y-12 Lot 13-5 Santa Maria coke flour,

discussed above in Section IB; Great Lakes Grade 1074 graphite flour; Airco-Speer KX-88 ("Nuclear No.2") graphite flour; and Airco-Speer Grade S-97 graphite flour, BBL58-2. Particle characteristics of the Santa Maria flour are listed in Table I, and those of the other three flours in Table XIX.

In Figs. 13 and 14, the particle-size distribution of Great Lakes Grade 1074 flour is compared with that of Santa Maria Lot 13-5. The usual tendency of the Santa Maria flour toward a bimodal distribution is evident. The 1074 flour shows a similar tendency, with the "hole" in the distribution in the same region of particle sizes. However, 1074 is a coarser flour, with much less material in the size range below about 10μ and much more in the range above about 40μ . Helium densities, surface areas, and fuzziness ratios indicate that the 1074 particles are relatively dense and contain less surface-connected porosity than do the Lot 13-5 Santa Maria particles.

TABLE XIX
PARTICLE CHARACTERISTICS
OF COMMERCIAL GRAPHITE FLOURS

	Grade		
	1074	KX-88	S-97
Helium Density, g/cm ³	2.217	2.172	2.209
Micromerograph Statistics (a)			
\bar{x}_3	3.182	3.242	3.206
s_{x3}^2	1.014	0.800	0.755
\bar{x}	0.382	0.129	0.525
s_x^2	0.175	0.216	0.266
\bar{d}_3 , microns	34.41	33.50	32.50
s_{d3}^2 , microns ²	487.8	339.6	348.0
\bar{d} , microns	1.685	1.35	2.06
s_d^2 , microns ²	2.447	2.27	4.79
g_d	48.3	46.4	96.4
S_W , cm ² /g	2167	1946	1809
CV_d	0.93	1.11	1.06
BET Surface Area			
S_W , m ² /g	11.65	8.72	5.24
s_S	0.18	0.10	0.07
d_s (b)	0.23	0.32	0.52
Fuzziness Ratio (c)	53.8	44.8	29.0

(a) Interval model.

(b) $d_s = 6/\rho S_W$.

(c) BET surface area divided by that calculated from Micromerograph data.

Microscopic examination showed a larger domain size in the 1074 particles, and greater acicularities, particularly of the finer particles.

Micromerograph particle-size data for the two Airco-Speer flours are plotted in Fig. 15. Neither sample distribution is lognormal, although their departures from lognormality are less extreme than those of the 1074 and 13-5 flours. Microscopically, the S-97 particles were

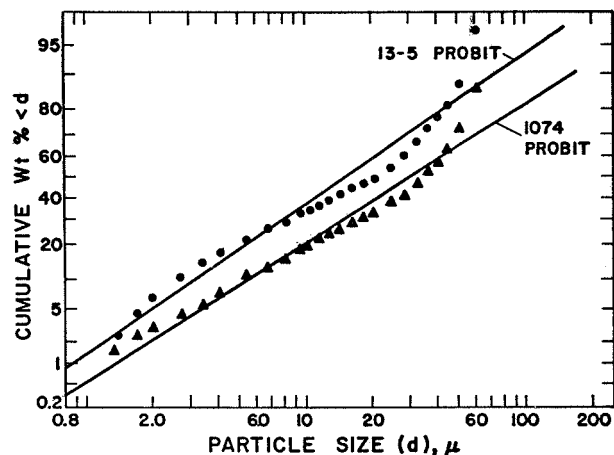


Fig. 13. Cumulative plot of Micromerograph particle-size data for Great Lakes 1074 and Santa Maria Lot 13-5 fillers.

observed to have lamellar internal structures with large domain sizes, and a tendency toward very acicular shapes, especially in the fine sizes. KX-88 particles were less acicular and had finer, more nearly random domain structures than either the S-97 or the 1074 flours. Although the KX-88 flour was slightly coarser than the S-97 flour, the two had very similar particle-size distributions. Surface area data indicated a greater amount of surface-connected porosity in the KX-88 flour.

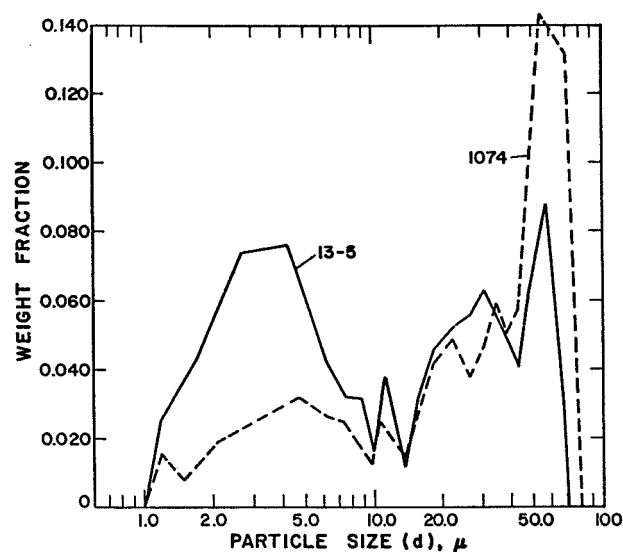


Fig. 14. Weight-fraction plot of same data shown in Fig. 13.

TABLE XX
COMPOSITION AND EXTRUSION CONDITIONS OF EXTRUDED RESIN-BONDED GRAPHITES

Specimen Number	Filler Flour Used	Amount pph	Binder		Extrusion Conditions				
			Identification	Viscosity, cp	Pressure, psi	Velocity in./min	Vacuum Torr	Temperature, °C	
ACX 1	G-26	25	QX 247	880	11475	153	450	44	45
ACX 2	G-18	27	QX 247	880	7200	161	450	40	45
ACX 3	G-26	26	QX 248	2000	11700	160	500	47	47
ACX 4	G-18	27.5	QX 248	2000	7740	156	450	36	45
ACX 5	G-26	25	EMW 305	960	7740	150	450	42	45
ACX 6	G-18	27	EMW 305	960	7200	154	450	46	45
ACX 7	G-26	25	EMW 304	2050	11925	160	450	49	48
ACX 8	G-18	27	EMW 304	2050	8325	160	450	49	50
ACE 3	G-18	27	EMW 1600	1600	7900	164	300	55	48
ACE 4	G-18	27	EMW 1600	1600	9000	151	350	60	50
ACE 8	G-18	27	EMW 1400	1400	---	171	1000	56	51
AAP 31	G-18	27	Varcum 8251	200	5625	171	500	54	51
ACI 4	G-26	25	Varcum 8251	200	6750	171	300	65	53
ACI 7	G-26	25	EMW 1600	1600	9000	171	600	52	52
ACI 11	G-26	25.5	EMW 1400	1400	---	171	350	40	57

B. Binders

1. Evaluation of Quaker Oats Resins (J. M. Dickinson)

As has been discussed in several previous reports, it is desirable that a furfuryl alcohol resin binder to be used in the manufacture of extruded graphites have a relatively small content of monomer-size molecules and a narrow molecular-size distribution, with a mean size in the medium to large region of molecular sizes. In general such a binder has a relatively high viscosity, although this must be controlled according to the fabrication procedures used.

The Quaker Oats Co. has manufactured two experimental resins to meet these general requirements. They are identified as "QX 247" and "QX 248," and have been described in Report No. 15 (pp 20-21) and in Table XIII of this report. In general they have somewhat broader molecular-size distributions than do CMB-13 ("EMW") resins of similar viscosity, represented by larger variances and coefficients of variation of their size distributions. For both the Quaker Oats and the CMB-13 resins,

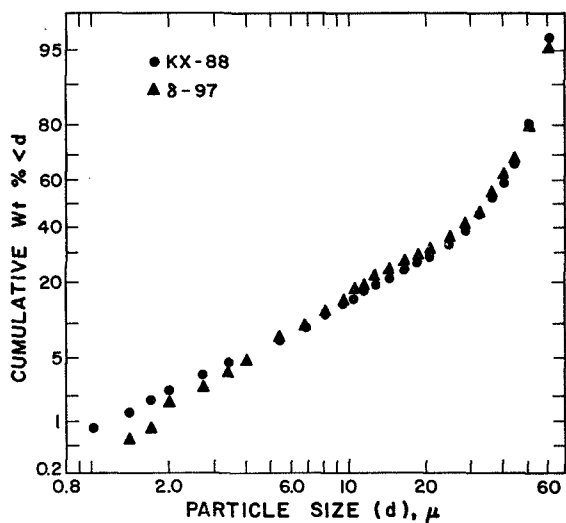


Fig. 15. Cumulative plot of Micromerograph particle-size data for Airco-Speer KX-88 and S-97 graphite flours.

TABLE XXI
PROPERTIES OF GRAPHITES MADE WITH SEVERAL HIGH-VISCOSITY RESINS

Specimen Number	Binder Used	Binder Viscosity, cp	Flour Used	Bulk Density, g/cm ³	Carbon Residue, %	Electrical Resistivity, $\mu\Omega$ cm	Young's Modulus, 10 ⁶ psi
ACX 1 ^(a)	QX 247	880	G-26	1.853	46.6	1742	1.57
ACX 5	EMW 305	960	G-26	1.907	49.6	1621	1.82
ACI 11 ^(a)	EMW 1400	1400	G-26	1.899	51.5	1645	1.73
ACI 7	EMW 1600	1600	G-26	1.906	50.2	1368	1.79
ACX 3	QX 248	2050	G-26	1.899	50.2	1653	1.81
ACX 7 ^(a)	EMW 304	2000	G-26	1.899	48.6	1700	1.78
ACI 4	Varcum 8251	200	G-26	1.863	47.6	1626	1.75
ACX 2	QX 247	880	G-18	1.893	48.5	1147	2.58
ACX 6	EMW 305	960	G-18	1.910	49.5	1158	2.64
ACE 8	EMW 1400	1400	G-18	1.927	50.2	1122	2.71
ACE 3	EMW 1600	1600	G-18	1.908	49.5	1105	2.57
ACE 4	EMW 1600	1600	G-18	1.918	50.6	1089	2.72
ACX 4	QX 248	2050	G-18	1.920	49.4	1125	2.71
ACX 8	EMW 304	2000	G-18	1.927	50.2	1122	2.71
AAP 31	Varcum 8251	200	G-18	1.876	46.6	1170	2.52

(a) Cracked.

the distributions tend to be skewed slightly toward the larger molecular sizes. This is not true of Varcum 8251 resin, whose distribution is skewed considerably toward the monomer end.

These resins were used to make the ACX series of graphites listed in Table XX, which, for comparison with graphites previously made from other resins, were extruded as 0.5-in. dia rods. The fillers used were Great Lakes Grade 1008-S graphite flour (CMB-13 Lot G-18), and Santa Maria graphite flour (CMB-13 Lot G-26, Y-12 "Blend 1"). Thermax carbon black was added in the proportion 15 parts Thermax to 85 parts graphite flour. Normal mixing, extrusion, and heat-treating procedures were used, except that curing was done by heating to 400°C at the relatively low rate of 2.5°C/hr. Final graphitization was at 2750 to 2800°C. Manufacturing data are listed in Table XX. Characteristics of the binders used are given in Table XIII.

In general, the extrusion pressures required were higher for mixes containing the Santa Maria (G-26) flour than for those containing the Great Lakes (G-18) flour, probably because of the blockier particle shapes and lower binder requirement of the Santa Maria filler. Binder requirements were slightly higher for the Quaker Oats resins than for the CMB-13 resins.

Properties of the ACX graphites and of others made using the same fillers and manufacturing procedures are listed in Table XXI. Specimen ACX1, which contained fine cracks, was made from too dry a mix. The properties listed for it may therefore be misleading.

High-quality graphites can evidently be made from either the Santa Maria or the Great Lakes filler using either the Quaker Oats or the CMB-13 binders. The properties of graphites made with any of the high-viscosity binders are definitely superior to those of similar graphites made with Varcum 8251. At similar viscosities, the CMB-13 binders gave slightly higher densities

TABLE XXII
CHARACTERISTICS OF CARBON RESIDUES FROM HEAT-TREATMENT OF POLYPHENYLENES

Polyphenylene No.	Heat-Treat Temp., °C	X-Ray Parameters			Carbon Yield, %
		Packed Density, g/cm ³	L _c , Å	d ₀₀₂ , Å	
1	850	0.332	10	3.49	86
	2850	0.319	120	3.40	83
	3100	0.288	160	3.40	--
1, Hot-Pressed	900	0.970	14.3	3.47	--
	2820	0.927	130	3.41	--
	3110	0.958	140	3.41	--
1, Rapid Htng.	2885	0.326	140	3.40	91
2	850	---	---	---	82
	2850	0.885	67.3	3.44	80
3	850	---	---	---	74
	2850	0.986	83.3	3.41	72

than did the Quaker Oats binders. Particularly for graphites made from the G-26 (Santa Maria) filler, there is a strong correlation between bulk density and the coefficient of variation of the binder's molecular-size distribution. In furfuryl alcohol resin binders, a low coefficient of variation is evidently desirable.

2. Synthesis of γ -BL (E. M. Wewerka, R. J. Barreras)

A complete reaction scheme for the synthesis of 4-methyl-4-furfuryl-2-en- γ -butyrolactone (" γ -BL"), a component of furfuryl alcohol resins prepared by polymerization with γ -alumina, was outlined in Report No. 14 of this series. At the time Report No. 15 was written, furfuryl methyl ketone (product No. 4) had been successfully synthesized, but the following product, an acetylide, had not.

During the preparation of furfuryl methyl ketone for further studies, it was determined that iron and hydrochloric acid gave higher product yields from nitroolefin than did the zinc and hydrochloric acid combination previously used. In the future the iron-hydrochloric acid procedure will be used for this step.

Attempts to react acetylide ion with furfuryl methyl ketone using sodium acetylide in liquid ammonia were unsuccessful. The use of a complex of lithium acetylide and ethylenediamine in tetrahydrofuran was successful,

and the desired acetylide (product No. 5) was isolated as a light-yellow, high-boiling liquid.

The further reaction of the acetylide product to γ -BL has not so far been accomplished.

3. Polyphenylene Binders (E. M. Wewerka)

In a continuing investigation of the potential usefulness of polyphenylenes as binders and carbon precursors, three different polyphenylenes have been synthesized and examined.

Polyphenylene No. 1 is a homopolymer of benzene, in which the predominant chain linkages are presumably at the para ring positions. Examination of the carbon residue from it after the heat-treatments listed in Table XXII gave no evidence that it had fused. Even after heat-treatment to 3100°C, the residue remained as unfused particles whose general appearance was not unlike that of the original polymer particles. To verify its infusibility, another sample of polyphenylene No. 1 was hot-pressed to 900°C under pressure of 4000 psi. As is indicated by column 3 of Table XXII, the hot-pressed material packed to much higher density in the x-ray sample-holder than did the first sample, but graphitized to about the same degree and again appeared not to have fused. A third sample of polyphenylene No. 1 was heated rapidly from room temperature to 2885°C, and behaved very

much like the first sample. The measured carbon yield from the third sample, 91%, seems unreasonably high. However, carbon yields of 83 and 86% from the first sample are high enough to make this polyphenylene interesting as a carbon precursor. In spite of the fact that it apparently does not fuse during carbonization, its residue graphitizes reasonably well, apparently because of a high degree of structural alignment in the original polymer structure. Because of its infusibility, this polyphene does not appear to be a candidate for use as a binder. However, it has obvious possibilities as a precursor for the manufacture of a synthetic filler.

Polyphenylene No. 2 is a copolymer of biphenyl and m-terphenyl. It was expected that its molecular arrangement would be much more random than that of polyphenylene No. 1, and that it might therefore be fusible. Indeed, after heat-treatment to 850°C, its residue was a mass of fused particles. Its carbon yield was also high, about 80% after heat-treatment to 2850°C, but the residue graphitized less well than did that from polyphenylene No. 1. The polymer itself was essentially amorphous, and its residue would probably be considered a carbon rather than a graphite even after high-temperature heat-treatment. Polyphenylene No. 2 is of interest principally because its behavior indicates that the general method of increasing fusibility by synthesizing irregularities into the polymer structure is effective.

Polyphenylene No. 3 is a homopolymer of biphenyl, and was expected to be quite similar to polyphenylene No. 1. X-ray diffraction measurements indicated that the structures of the two polymers were similar, each containing about 25% of crystalline material. However, after heat-treatment to 850°C polyphenylene No. 3 was found to be a fused foam-like mass. Carbon yield was considerably lower than those of the other two polyphenylenes, and the crystallite size produced by heating the residue to 2850°C was much smaller than was the case for No. 1. These differences suggest that, in spite of the x-ray evidence, the structure of polyphenylene No. 3 was much more disordered than that of No. 1. It is probable that much of the disorder was produced by fusion of the

TABLE XXIII
VISCOSITIES OF UNDILUTED AND DILUTED
FURFURYL ALCOHOL RESINS

<u>Resin No.</u>	<u>Original Viscosity, cp</u>	<u>Diluted Viscosity, cp</u>	<u>Ratio of Viscosities</u>
EMW 303	1,440	410	3.5
EMW 304	2,160	550	3.9
EMW 311	3,900	800	4.9
EMW 312	13,000	2,200	5.9
EMW 313	29,500	3,600	8.2
EMW 310	50,000	5,900	8.5

polymer during carbonization, but it is not clear why No. 3 fused while No. 1 did not.

4. Viscosity Measurements (E. M. Wewerka)

Accurate measurements of the viscosities of furfuryl alcohol resins are made difficult by two resin characteristics: their relatively large temperature coefficients of viscosity, and their occasional thixotropic or non-newtonian behaviors. Temperature effects can be avoided simply by insuring that temperature is uniform throughout the resin when the measurement is made and that all measurements are made at the same temperature. Thixotropy, however, is much more difficult to control, because it is not well understood. It seems to come and go according to such factors as the final temperature to which a resin has been heated during polymerization or stripping, the rate at which it was cooled to room temperature, and the amount of agitation to which it was subjected before a viscosity measurement was made. The same resin may, unpredictably, be thixotropic or not, and so may give widely different viscosity values. This of course makes it very difficult to correlate viscosity data either within a single laboratory or between laboratories.

CMB-13 has so far had little difficulty with inconsistencies in viscosity measurements arising from thixotropy effects, apparently because the handling of the experimental resins made here has been nearly identical from batch to batch. If viscosity measurements have been affected by thixotropy, the effect has at least been

TABLE XXIV
EFFECTS OF TEMPERATURE ON RESIN VISCOSITIES

Resin No.	Viscosity in Centipoises at					
	25°C	30°C	35°C	40°C	45°C	75°C
EMW 311	3900	2500	1620	1000	680	82
EMW 313 plus 10% furfural	3600	2500	1600	1000	720	75

a consistent one. Quaker Oats Co., using a variety of preparative techniques, reports continual difficulties from it. It has been suggested that the tendency of a resin to exhibit thixotropic behavior may be reduced if it is diluted slightly with a solvent prior to the viscosity measurement. The Quaker Oats chemists are therefore interested in the possibility of reporting the viscosities of furfuryl alcohol resins in an "as-diluted" condition.

To examine the feasibility of measuring and reporting viscosities in this way, viscosities were measured on a group of CMB-13 resins before and after diluting them with 10% by weight of furfural. The resins used were acid-polymerized furfuryl alcohol resins ranging in viscosity from 1400 to 50,000 cp. Results are listed in Table XXIII. From the ratios of original viscosities to those measured after dilution, it is evident that the effect of the solvent addition increases with the viscosity of the resin. Since the Quaker Oats chemists have found that the higher viscosity resins are more subject to anomalous thixotropic behavior, this trend is desirable. Dilution of these resins with solvent prior to viscosity measurement does appear to be advantageous, at least to the degree that it reduces uncertainties arising from thixotropy. Its effectiveness in doing this is now being investigated at Quaker Oats Co.

Typically, the temperature coefficient of viscosity of a furfuryl alcohol resin is very high. If this were affected by dilution of the resin with furfuryl, then a viscosity measurement on the diluted resin would be meaningful only at the precise temperature at which the measurement was made. To investigate this, viscosity measurements were made at a series of temperatures on the two acid-polymerized CMB-13 resins listed in Table XXIV. Resin EMW 311 had a viscosity of 3900 cp at 25°C. Resin EMW

313, after dilution with 10% furfural, had a viscosity of 3600 cp at 25°C. Viscosities of the undiluted and diluted resins remained nearly equal as they were heated over the temperature range 25 to 75°C. It appears that dilution of a furfuryl alcohol resin with a solvent has very little effect on its temperature coefficient of viscosity.

5. Temperature-Dependence of Viscosity (E. M. Wewerka)

As has been discussed in several previous reports, a furfuryl alcohol resin produced by polymerization with γ -alumina differs significantly in molecular composition from an acid-polymerized resin. In the early work on such resins at Armour Research Foundation, one of the advantages claimed for the alumina-polymerized resin was that it decreased in viscosity more rapidly as temperature increased than did an acid-polymerized one, facilitating mixing and fabrication when it was used as a binder.

This was investigated by measuring the viscosity of a CMB-13 resin prepared by polymerization with γ -alumina, over the temperature range 25 to 100°C. Data are plotted in Fig. 16, together with similar data for an acid-polymerized resin. On a log-log plot, viscosity of the alumina

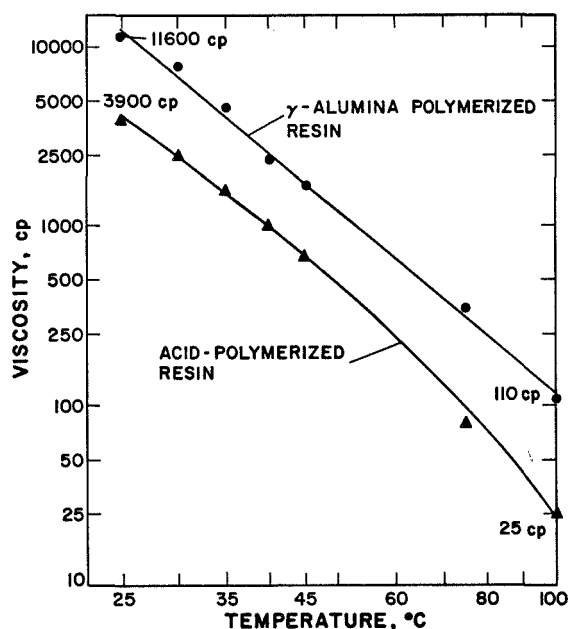


Fig. 16. Effects of temperature on the viscosities of furfuryl alcohol resins produced by polymerization with γ -alumina and with an acid catalyst.

TABLE XXV
EXTRUSION CONDITIONS FOR ADC GRAPHITES

Specimen Number	Die Diameter, in.	Mandrel Diameter, in.	Half-Thickness, in. (a)	Surface-to-Volume Ratio (a)	Extrusion Conditions				
					Pressure, psi	Velocity, in./min	Temperature		Vacuum, Torr
							Mix, °C	Chamber, °C	
ADC 1	0.625	---	0.312	6.4	6750	110	37	43	400
ADC 2	0.625	0.25	0.187	10.6	5940	141	36	45	500
ADC 3	0.625	0.1	0.262	7.6	7020	114	40	48	450
ADC 4	0.5	---	0.25	8.0	5400	157	34	45	500
ADC 5	0.5	0.25	0.125	16.0	7065	225	35	47	500
ADC 9	0.5	0.1	0.2	10.0	6750	180	36	48	500
ADC 7 ^(b)	0.25	---	0.125	16.0	10000	240	37	45	500
ADC 8 ^(b)	0.25	0.1	0.075	26.7	11800	220	36	48	500

(a) Based on die and mandrel sizes.

(b) Average values for several extrusion batches.

polymerized resin is nearly linear with temperature, and the temperature-dependence is essentially the same as that shown by the Armour data. Within the data scatter, the temperature-dependence of the viscosity of the acid-polymerized resin appears to be very similar to that of the alumina-polymerized resin.

VI. MANUFACTURING VARIABLES

A. Size and Shape Effects (J. M. Dickinson)

Most of the properties of a graphite depend directly on its bulk density, which is strongly affected by the carbon yield realized from pyrolysis of the binder. Carbon yield is controlled by a combination of factors, including the molecular composition and distribution of the binder, heating rates and the gaseous environment during polymerization and pyrolysis, and the characteristics of the filler system with which the binder is associated. All of these factors have previously been investigated in some detail. However, carbon yield is also affected by the residence time of pyrolysis gases within the formed body, which is a function of its size and shape. This has not previously been investigated systematically.

To explore the effects of size and shape, a series of extruded graphite rods and tubes was made from a mix

containing 85 parts Great Lakes Grade 1008-S graphite flour (CMB-13 Lot G-18), 15 parts Thermax carbon black, and 27 parts Varcum 8251 furfuryl alcohol resin catalyzed with 4% maleic anhydride. Solid rods were extruded in dies having nominal diameters of 5/8, 1/2, and 1/4 in. Extruded tubes having these same outside diameters were produced by inserting 1/4- and 1/10-in. dia mandrels into the dies. Extrusion conditions are summarized in Table XXV. Curing, baking, and graphitizing were done in normal cycles except that--due to furnace trouble--graphitization was to only 2680°C. Since there is very little loss of binder carbon above about 2500°C and since all samples were heat-treated together, this is believed not to have affected the experimental results.

Although die geometries were similar throughout, the use of the same 2-in. dia materials chamber for all die sizes, with and without mandrels, resulted in widely different extrusion ratios for the various rods and tubes. However, there appeared to be no correlation between reduction of area and carbon yield. There did appear to be a trend toward lower carbon yield as extrusion pressure was increased. This was unexpected, since higher extrusion pressure normally increases bulk density. In this case, the correlation of bulk density (Table XXVI)

TABLE XXVI
P PROPERTIES OF ADC GRAPHITES

Specimen Number	Batch Number	Bulk Density, g/cm ³	Carbon Residue			Electrical Resistivity, $\mu \Omega$ cm	Young's Modulus, 10 ⁶ psi
			Cured %	Baked %	Graph. %		
ADC 1		1.868	85.6	49.8	48.6	1122	2.51
ADC 2		1.856	83.6	47.5	46.2	1127	2.45
ADC 3		1.893	85.2	49.4	48.1	1136	2.44
ADC 4		1.871	85.7	47.5	46.1	1132	2.45
ADC 5		1.864	84.2	45.7	44.2	1132	2.38
ADC 9		1.879	85.8	48.4	46.9	1219	2.51
ADC 7	1	1.792	81.0	42.4	40.9	1552	2.03
ADC 7	2	1.802	82.5	43.9	42.3	1511	2.15
ADC 7	3	1.829	83.1	45.0	43.5	1489	2.26
ADC 7	Avg. (a)	1.818	82.8	44.5	42.9	1500	2.19
ADC 8	1	1.784	78.4	39.8	37.8	1661	2.00
ADC 8	2	1.800	79.3	41.0	39.4	1656	2.01
ADC 8	3	1.811	80.7	42.2	40.6	1610	2.12
ADC 8	4	1.808	81.1	42.7	40.9	1632	2.09
ADC 8	Avg. (a)	1.810	80.9	42.4	40.7	1621	2.10

(a) Average for batches selected to represent the most desirable extrusion conditions tried.

with extrusion pressure was poor, and carbon yield varied with bulk density.

As an indication of the length of the escape path for pyrolysis gases, a length equal to one-half of the section thickness for each specimen geometry has been listed in Table XXV. The surface-to-volume ratio for each geometry has also been listed, as an indication of the relative area available for escape of pyrolysis gases. Other properties of the various extrusions are listed in Table XXVI.

Figure 17 demonstrates the strong effect of surface-to-volume ratio on the yield of binder carbon in both rods and tubes. An increase in this ratio, representing an increase in the area through which a given volume of pyrolysis gases can escape, reduces the proportion of binder carbon retained in the solid body. Presumably this results from reduced residence time of pyrolysis gases within the fine void structure of the body, where time-dependent reactions can occur that result in deposition of carbon on the walls of the voids.

The effect of section thickness on binder-carbon yield is illustrated in Fig. 18, where the abscissa represents the distance from the center of the section to the nearest free surface. As the distance through which the

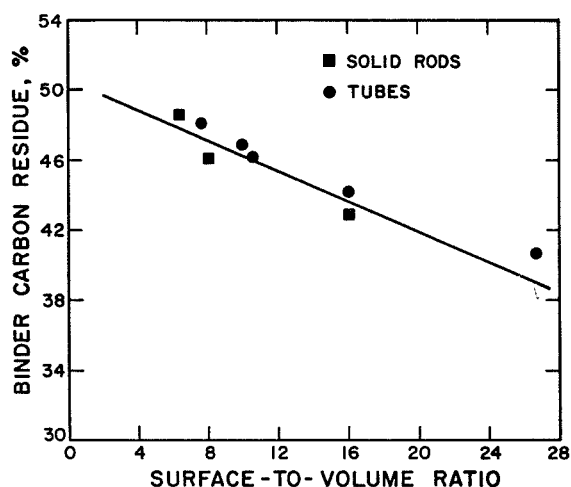


Fig. 17. Effect of surface area-to-volume ratio on binder-carbon yield in extruded tubes and rods.

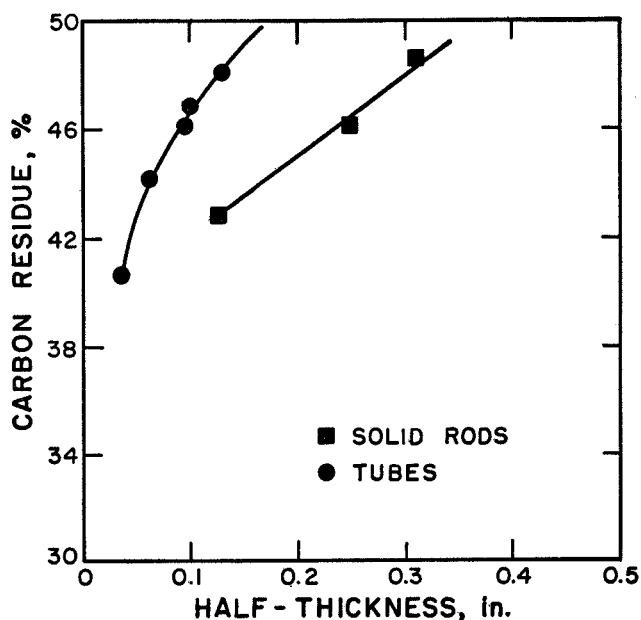


Fig. 18. Effect of section thickness on binder-carbon yield in extruded tubes and rods.

pyrolysis gases must travel to escape from the body increases, so does the proportion of binder carbon left behind. However, separate curves are required to represent the behaviors of rods and of tubes. In the case of a cylindrical rod, the area through which gas can flow from any internal point increases continuously toward the free surface of the rod, through which it must eventually escape. In the case of a cylindrical tube, this is true only toward the outer surface. Toward the inner surface of the tube the area of the flow path decreases, and impedance to gas flow increases. At the same section thickness, the average impedance to gas flow is greater for the tube than for the rod, residence time of the gases is longer, and carbon residue is higher. As section-thickness increases so does carbon residue, but, because of the geometry of the gas-flow path, the increase is more rapid for the tube than for the rod.

It is evident that, to increase carbon yield and bulk density, it is desirable to increase the residence time of pyrolysis gases within the body. This can be done by reducing the surface-to-volume ratio of the shape produced, and increasing the section thickness.

It is also evident that, if a particular shape is to be mocked up successfully by a smaller or simpler one, there must be a careful matching of surface-to-volume

ratios, section thicknesses, and geometries of the gas-escape paths.

VII. POROSITY EFFECTS

A. Previous Work

The effects of porosity on the properties of graphites have previously been discussed in Reports 11-15 in this series.

B. Mercury Porosimetry (J. M. Dickinson)

Much of the work previously reported on the relations between the porosity of a graphite and its properties has been done on the group of POCO graphites listed in Table XXVII, all of which were heat-treated together in flowing helium at 2900°C. The porosities of these materials have been further examined by mercury porosimetry, with the results shown in the table.

Porosimetry data are similar for most of the graphites, and indicate that in general the pores are small and highly interconnected. Specimens 6 and 7, which had been impregnated by the manufacturer, have much smaller pore sizes and more inaccessible porosity than do the unimpregnated graphites. Specimens 3 and 4, which had been impregnated and regraphitized by the manufacturer, were intermediate in both pore size and pore accessibility between specimens 6 and 7 and the other graphites. The variance and skewness of the pore-size distributions of the two graphites that had been impregnated and regraphitized were extremely low, indicating that this post-manufacturing treatment was effective in obstructing the coarser pores. The corresponding statistics for Specimens 6 and 7, which had been impregnated but not regraphitized by the manufacturer, were much like those of unimpregnated samples. This is unexpected since, like all other specimens listed, these were graphitized to 2900°C by CMB-13 before the porosimetry measurements were made.

Specimen 15 was investigated up to a mercury pressure of 15,000 psi as well as to the usual pressure of 2600 psi. At the higher pressure nearly all of the porosity of the graphite was intruded by mercury, suggesting

TABLE XXVII
MERCURY-POROSIMETRY DATA, HEAT-TREATED POCO GRAPHITES

Specimen No.	Original POCO Grade	Bulk Density, g/cm ³	Porosity, %			Pore-Size Distribution Statistics (a)		
			Total	Accessible to Hg at 2600 psi	Inaccessible to Hg at 2600 psi	Mean Pore Dia, $\mu \bar{d}_3$	Variance of Distribution, $s_{d_3}^2$	Skewness of Distribution, g_{d_3}
15 ^(b)	AXZ-9Q	1.539	31.6	30.3	1.3	0.97	7.86	300
14	AXZ	1.544	31.4	30.4	1.0	1.05	11.04	452
5	AXZ-QBG	1.625	27.8	---	---	---	---	---
8	AXZ-QB	1.631	27.5	---	---	---	---	---
11	EP-1924	1.753	22.1	19.9	2.2	1.05	11.03	435
12	AXM-5Q	1.755	22.0	19.3	2.7	1.06	14.25	601
10	EP-1924	1.766	21.5	16.7	4.8	1.20	19.87	852
13	AXM-5Q	1.767	21.4	18.5	2.9	---	---	---
9	EP-1924	1.773	21.2	18.3	2.9	1.23	19.96	848
2	AXF-5Q	1.788	20.5	---	---	---	---	---
1	AXF-5Q	1.817	19.2	---	---	---	---	---
3	AXF-QBG	1.834	18.5	13.0	5.5	0.66	0.21	1.19
6	AXF-QB	1.896	15.7	9.2	6.5	0.74	18.91	738
4	AXF-QBG	1.900	15.6	10.7	4.9	0.52	0.09	0.01
7	AXF-QB	1.904	15.4	8.8	6.6	0.78	13.10	540

(a) Finite-interval calculation.

(b) At 15,000 psi, accessible porosity of this specimen was 31.4% and inaccessible porosity was 0.2%.

considerable internal damage to the graphite structure. However, the pore-size distribution statistics derived from this high-pressure run were nearly the same as those from a normal-pressure run, indicating that the additional pores which were opened by high pressure are very much like those which are accessible to mercury at low pressure.

C. Helium Pycnometry (H. D. Lewis)

The AFA-4 surface-area analyzer was modified and calibrated to make helium-pycnometer density measurements on the 3-in. long, 0.5-in. dia specimens used for elastic-modulus measurements. Data collected on the 15 POCO graphite specimens discussed above are listed in Table XXVIII. As would be expected, the porosity inaccessible to helium was consistently less than that which was inaccessible to mercury. However, the differences are not large.

Specimens 5 and 8 presumably represent the relatively low-density AXZ grade, impregnated and, respectively, regraphitized and not regraphitized. The impregnation treatment has significantly increased both bulk density and the porosity that is inaccessible to helium. However, in neither respect are these materials equivalent to unimpregnated grades of higher initial density.

D. Gas Permeability (P. Wagner)

Permeabilities of these POCO graphites to nitrogen were measured using a modified Ruska permeameter, with the results listed in Table XXVIII. Permeabilities were generally low, and were significantly reduced by impregnation. Specimens 3, 4, 6, and 7, which were impregnated high-density grades, had permeabilities too low to be measured with this apparatus.

TABLE XXVIII

POROSITY AND PROPERTIES DATA, HEAT-TREATED POCO GRAPHITES

Specimen Number	Helium Density, g/cm ³	Porosity Inaccessible to Helium, %	Nitrogen Gas Permeability, millidarcys	CTE, x 10 ⁻⁶ /°C		Lorenz Function x 10 ⁻⁸ v ² /K ²
				Average 25-645°C	At 645°C	
15	2.232	0.6	2.20	7.44	8.79	470
14	2.237	0.4	2.15	7.11	8.19	490
5	2.224	0.9	0.46	7.24	8.61	490
8	2.214	1.2	0.45	7.07	7.92	400
11	2.204	1.6	0.53	7.07	8.71	420
12	2.186	2.3	0.50	7.44	9.16	510
10	2.179	2.6	0.26	7.61	9.07	480
13	2.178	2.6	0.43	7.23	8.60	530
9	2.202	1.7	0.31	7.89	8.97	460
2	2.177	2.7	0.39	7.98	9.08	460
1	2.178	2.7	0.25	7.69	8.61	540
3	2.145	4.0	<0.1	6.92	7.62	490
6	2.101	6.0	<0.1	7.68	9.15	---
4	2.127	4.9	<0.1	7.78	8.47	---
7	2.099	6.1	<0.1	7.33	8.66	580

E. Thermal Expansion (P. Wagner)

The thermal expansion coefficients ("CTE's") listed in Table XXVIII were measured in a nitrogen atmosphere using a quartz dilatometer. For each specimen an average CTE value over the interval 25 to 645°C is listed, together with a value measured at the top of this interval, 645°C.

The mean of the average CTE's is $7.43 \times 10^{-6}/^{\circ}\text{C}$ over this temperature range, with a standard deviation of 4.2%. Since this uncertainty is within the measurement precision of the apparatus, it is concluded that for this series of graphites the CTE is independent of density. This agrees with the conclusion of Engle (Carbon 8, 485, 1970), and disagrees with that of Sutton and Howard (J. Nucl. Mat. 7, 58, 1962)--who made a strong case for internal accommodation of thermal expansion by voids in the graphite structure.

For instantaneous values of CTE measured at 645°C, the average is $8.64 \times 10^{-6}/^{\circ}\text{C}$, with standard deviation of 5.1%. At the same temperature, single-crystal values are $28 \times 10^{-6}/^{\circ}\text{C}$ in the c-direction and $0.5 \times 10^{-6}/^{\circ}\text{C}$ in

the a-directions, so that the calculated CTE for a theoretically dense isotropic graphite is $9.7 \times 10^{-6}/^{\circ}\text{C}$.

Values for commercial polycrystalline graphites are generally in the neighborhood of $4 \times 10^{-6}/^{\circ}\text{C}$. The average value for this series of POCO graphites ($8.64 \times 10^{-6}/^{\circ}\text{C}$) is only 11% lower than the theoretical value. The difference can probably be accounted for by internal restraints on expansion, without invoking an internal accommodation mechanism. On the other hand, from the helium-inaccessible porosities listed in Table XXVIII, it appears that the closed porosities in this series of graphites ranged only from 0.4 to 6.1% of the specimen volume. If it is assumed that the closed porosity includes the cracks formed by restrained thermal contraction ("Mrozowski cracks") and that only such cracks can accommodate thermal expansion, then it can probably be argued that this range of crack volumes was simply too small to have an observable effect on the measurements here described.

TABLE XXIX
EXPERIMENTAL GRAPHITES TESTED IN THERMAL SHOCK

Specimen No.	Filler	Binder	Density, g/cm ³	Comments
ACS 4	G-26 ^(a)	EMW 10	1.710	Appears binder deficient. Many equiaxed pores.
ACS 1	G-26	EMW 250	1.847	Dried out excessively during extrusion. Much porosity.
ACS 2	G-26	EMW 250	1.895	Elongated pores less than 50 μ long.
ACI 7	G-26	EMW 1400	1.906	Elongated pores up to 400 μ long, highly oriented near surface.
ACS 5	G-26	EMW 1400	1.912	Some elongated pores up to several hundred microns long, parallel to extrusion axis.
ACR 2	G-18 ^(b)	V 8251	1.855	Very few elongated pores.
ACA 2	G-18	V 8251	1.878	Elongated pores up to 150 μ long with some orientation parallel to axis.
ACE 3	G-18	EMW 1600	1.893	Elongated pores 60-70 μ long; some circumferential voids near surface.
ACR 1	G-18	EMW 1600	1.896	Very few elongated pores.
AAQ 1	G-13 ^(b)	V 8251	1.901	Very few elongated pores.
ACE 8	G-18	EMW 1400	1.914	Elongated pores up to 200 μ long with some orientation parallel to axis.
ACP 14	G-18	V 8251	2.695	Contains 19 vol % ZrC. Very few elongated pores.

(a) Santa Maria graphite flour.

(b) G-18 and G-13 are different lots of Great Lakes 1008-S graphite flour.

F. Lorenz Function (P. Wagner)

If it is assumed that all heat conduction in graphite is electronic in nature, as it is in metals, then thermal conductivity (λ) should be related to electrical conductivity (σ) and absolute temperature (T) by the equation $\lambda = L\sigma T$, where L is the Lorenz function. To see whether the degree of electronic heat conduction changed with porosity, values of L for the series of POCO graphites were calculated from room-temperature values of λ and σ . The L values are listed in Table XXVIII and, within the errors of the measurements involved, they did not change with porosity. The apparent independence of λ and P suggests that, in graphite, electron-scattering by pores is not important in thermal conduction, and supports the phonon-scattering mechanism previously proposed.

The average value of the Lorenz function for these graphites, about $490 \times 10^{-8} \text{ V}^2/\text{K}^2$, is approximately 200 times as great as the Lorenz function for metals.

As has previously been assumed, the mean pore diameters of these graphites (0.52 to 1.23 μ , by mercury porosimetry) are indeed large in comparison with the phonon wavelength of 0.008 μ (Kelly, Wagner, Tobin, and Whittaker, Carbon, in press). This is required for phonon-scattering by pores.

VIII. THERMAL-SHOCK RESISTANCE OF EXTRUDED, RESIN-BONDED GRAPHITES

(J. M. Dickinson)

The relative thermal-shock resistances of the eleven experimental graphites and one graphite-ZrC composite listed in Table XXIX have been measured by C. R. King, LASL Group N-7. The specimens used were washer-shaped, 0.5-in. dia and 1/16-in. thick, with a 0.25-in. dia axial hole. These were supported individually on a water-cooled mandrel extending through the axial hole, and heated very rapidly by radio-frequency currents

TABLE XXX
THERMAL SHOCK INDICES AND OTHER PROPERTIES OF GRAPHITES

Specimen No.	Thermal Shock Indices (a)	Bulk Density, g/cm ³	Young's Modulus, (b) 10 ⁶ psi	Resistivity, $\mu\Omega\text{cm}$		Coeff. of Thermal Exp. (c), $\times 10^{-6}/^{\circ}\text{C}$	
				WG	AG	WG	AG
ACS 4	145/147.5	1.710	---	2151	---	5.40	6.00
ACS 1	155/157.5	1.847	1.45	1823	---	5.63	6.01
ACS 2	180/182.5	1.895	1.72	1628	---	5.18	5.71
ACI 7	155/157.5	1.906	1.79	1368	1884	4.93	5.45
ACS 5	170/172.5	1.912	1.76	1619	---	5.33	5.70
ACR 2	170/172.5	1.855	---	1194	---	---	---
ACA 2	160/162.5	1.878	2.50	1144	2173	2.45	4.69
ACE 3	185/187.5	1.893	2.57	1105	2059	2.50	5.22
ACR 1	180/182.5	1.896	---	1160	---	---	---
AAQ 1	167.5/170	1.901	2.2	1160	1901	2.23	4.21
ACE 8	170/172.5	1.914	2.67	1091	---	---	---
ACP 14 ^(d)	157.5/160	2.695	3.97	348	---	---	---
SX5-1	150/152.5						
SX5-2	145/147.5						
CS-312	180/185						
RVC-1	175/177.5						
RVC-2	190/192.5						
H 205	190/192.5						

(a) Across-grain orientation.

(b) With-grain orientation.

(c) Average, 25-645°C.

(d) Composite, 19 vol % ZrC.

induced in a thin skin at the perimeter of the specimen. For each material a number of specimens were tested at a series of power settings on the high-frequency power supply. The pairs of numbers listed as thermal shock indices in Table XXX represent for each material the maximum power setting that did not cause specimens to fracture, and the minimum setting that caused essentially all of them to fracture. Since the specimens used were slices from 0.5-in. dia rods, the temperature gradient established in the test was radial relative to the original rod, and the thermal-shock indices therefore apply to the across-grain orientation of the material. The test is a

comparative one and, for comparison, the same test was applied to the commercial graphites listed at the bottom of Table XXX.

The experimental graphites tested were extruded from mixes containing either Great Lakes 1008-S (CMB-13 Lot G-18) or Santa Maria (Lot G-26) graphite flour filler and either Varcum 8251 or an experimental CMB-13 furfuryl alcohol resin binder. Fifteen pph of Thermax carbon black were added in all cases. These materials were selected because they contained no obvious manufacturing defects and covered a relatively broad range of

densities. Specimen ACP14 contained 19 vol % ZrC, and so was actually a graphite-matrix particulate composite.

The commercial graphites tested are pitch-bonded grades, of which SX5 and CS-312 are extruded and RVC and H205 are molded products. They range from poor to good in thermal-shock resistance. Several of the experimental graphites compared well with them in spite of the fact that all of the CMB-13 graphites were resin-bonded and were tested in their least-favorable orientation. Specimen ACS2 had relatively high thermal-shock indices for a near-isotropic, high-expansion graphite, and Specimen ACE3, made from a more acicular, lower-expansion flour, had an even higher thermal-shock rating. Both were bonded with high-viscosity experimental resins.

The three CMB-13 graphites which had high thermal-shock indices (above 180) had densities between 1.893 and 1.896 g/cm³ and contained elongated pores usually less than 60 μ long in the axial direction of the rod. All graphites contain voids, and thermal-shock resistance might be expected to increase with bulk density as the voids were eliminated. In the case of these graphites, it did not appear to increase when densities were greater than about 1.90 g/cm³. This may be because the voids present in the very high density extruded graphites tend to occur as elongated pores, sometimes several hundred microns long. These may join to form longitudinal microcracks which, particularly for the transverse directions, reduce resistance to thermal shock. Control of this void structure may offer a means of improving thermal-shock resistance.

IX. PUBLICATIONS RELATING TO CARBONS AND GRAPHITES

- Green, W. V., "Creep and Stress Rupture Testing," Chapter 6 in Techniques of Metals Research, Vol. 5, Part 1, Ed., Dr. R. F. Bunshah, John Wiley & Sons, Inc., p. 371-456, 1971.
- Smith, M. C., "CMF-13 Research on Carbon and Graphite, Report No. 15, Summary of Progress from August 1 to October 31, 1970," LA-4631-MS, February, 1971.